ISSN 0869-5911, Petrology, 2015, Vol. 23, No. 1, pp. 22–44. © Pleiades Publishing, Ltd., 2015.
Original Russian Text © A.A. Tretyakov, K.E. Degtyarev, K.N. Shatagin, A.B. Kotov, E.B. Sal'nikova, I.V. Anisimova, 2015, published in Petrologiya, 2015, Vol. 23, No. 1, pp. 26–49.

Neoproterozic Anorogenic Rhyolite–Granite Volcanoplutonic Association of the Aktau–Mointy Sialic Massif (Central Kazakhstan): Age, Source, and Paleotectonic Position

A. A. Tretyakov[a], K. E. Degtyarev[a], K. N. Shatagin[b], A. B. Kotov[c], E. B. Sal'nikova[c], and I. V. Anisimova[c]

[a]*Geological Institute, Russian Academy of Sciences, Pyzhevskii per. 7, Moscow, 119017 Russia*
e-mail: and8486@yandex.ru
[b]*Institute of Geology of Ore Deposits, Petrography, Mineralogy, and Geochemistry (IGEM), Russian Academy of Sciences, Staromonetnyi per. 35, Moscow, 119017 Russia*
e-mail: shat@igem.ru
[c]*Institute of Precambrian Geology and Geochronology, Russian Academy of Sciences, nab. Makarova 2, St. Petersburg, 199034 Russia*
e-mail: akotov@peterlink.ru

Received June 21, 2014

Abstract—Rhyolite–granite volcanoplutonic association was identified among the Precambrian basement complexes of the Aktau–Mointy Massif, Central Kazakhstan. This association comprises rhyodacites, rhyolites, subalkaline rhyolites, tuffs, and felsic volcanogenic-sedimentary rocks of the Altyn Syngan and Urkendeu formations, as well as granitoids of the Uzunzhal Complex. U–Pb (ID-TIMS) dating of accessory zircons from the volcanic rocks and granites showed that the association was formed in the Neoproterozoic (Tonian, 925–917 Ma). The Neoproterozoic volcanic rocks and granites are the youngest Precambrian magmatic complexes and mark the final stage in the formation of the Precambrian crust of the Aktau–Mointy Massif. In terms of major and trace element composition, the volcanic rocks and granites resemble A-type granites, thus indicating the within-plate settings of their formation. It was established that their primary magma could be derived by melting of metatonalitic or metagraywacke protolith at $T \geq 940°C$ and $P \sim 8–10$ kbar in response to mantle magma underplating. Sm–Nd isotope data on the volcanic rocks and granites ($T_{Nd}(DM) = 1.9–1.7$ Ma, $\varepsilon_{Nd}(T)$ from −1.9 to −3.5) testify the Paleoproterozoic age of their crustal protolith. Available data have revealed strong similarity between the Neoproterozoic tectonomagmatic evolution of the Aktau–Mointy Massif and the Congo–São Francisco paleocontinent, which, with other cratons, composed the southern Rodinia supercontinent. This suggests that the formation of the Tonian anorogenic volcanoplutonic association of the Aktau–Mointy sialic massif was related to the global-scale divergent processes in the southern Rodinia supercontinent (Congo–São Francisco paleocontinent).

DOI: 10.1134/S0869591115010063

INTRODUCTION

The main structural plan of the Central Asian Fold Belt (CAFB) is mainly determined by a combination of large Precambrian sialic massifs and intervening Paleozoic lithotectonic zones (Degtyarev and Ryazantsev, 2007; Degtyarev, 2012). The structure of the massifs is traditionally subdivided into the basement, which is made up of variably metamorphosed Proterozoic complexes, and unmetamorphosed Ediacaran–Lower Paleozoic terrigenous–carbonate cover (Degtyarev, 2003; Degtyarev and Ryazantsev, 2007, etc.). The basement of many massifs is composed of high-grade gneissic complexes and (or) weakly metamorphosed quartzite–schist sequences, which are ascribed, respectively, to the Paleo- and Neoproterozoic. It is suggested that the metaterrigenous quartzite–schist sequences were accumulated on the passive shelf margin of the Rodinia supercontinent, which also included sialic massifs of the western CAFB in the Late Precambrian.

One more distinctive structural feature of some Precambrian sialic massifs in the western CAFB is the wide development of felsic volcanic rocks, which are localized at different structural levels in the quartzite–schist sequences of the subplatform cover, and associated granitoids. Unfortunately, available data do not permit a sufficiently accurate estimation of their age, as well as determination of their tectonic setting and role in the formation of the Precambrian continental crust of the CAFB. In this paper, the results of geological, U–Pb geochronological, geochemical, and Sm–Nd isotope studies are presented for the pre-Ediacaran volcanic rocks and associated granites of the Aktau–Mointy sialic massif in Central Kazakhstan, one of the largest Precambrian massifs of the western CAFB.

GEOLOGICAL STRUCTURE OF THE AKTAU–MOINTY MASSIF

The Precambrian Aktau–Mointy sialic massif (Fig. 1) is located in the western part of Central Kazakhstan and represents the northwestern continuation of the Precambrian Dzhungar massif. The massif strikes in the northwestern direction for almost 800 km at a width of 150–200 km. The Aktau–Mointy Massif is thrust onto the Ordovician complexes of the Eremen-tau–Buruntau zone in the southwest and is unconformably overlain by Silurian terrigenous sequences of the Agadyr zone in the northeast (Degtyarev, 2003).

The Precambrian basement of the Aktau–Mointy Massif is made up of the greenschist-facies metamorphosed pre-Ediacaran terrigenous, volcanic and subvolcanic rocks, which are unconformably overlain by terrigenous–carbonate sequences of the terminal Precambrian–Ordovician. The Late Precambrian sequences are intruded by gneiss granite and granite plutons of the Uzunzhal Complex (Avdeev et al., 1974; Zaichkina et al., 1982; Filatova et al., 1988).

The structural plan of the eastern Aktau–Mointy Massif is mainly defined by large anticlines, with quartzite–schist sequences of the Kiik Group exposed in their cores. The base of the group is composed of weakly metamorphosed, slightly sheared mudstones, siltstones, quartz sandstones, and carbonaceous–clayey schists with marble lenses (Aikarly Formation up to 2000 m thick). Upsection, these rocks grade into quartzite-sandstones with interbeds and lenses of fine-pebble essentially quartzite conglomerates (Aktau Formation up to 1000 m thick). The metaterrigenous rocks of the Kiik Group are unconformably overlain by the volcanic rocks of the Altyn Syngan Formation over 2000 m thick. It is mainly made up of weakly metamorphosed coarse- and finely fluidal felsic lavas locally transformed into porphyroids, crystal tuffs, tuffaceous-sedimentary rocks, and subvolcanic granite porphyries. A bed of bouldery conglomerates with quartzite pebbles is traced at the base of the Altyn Syngan Formation (Avdeev, 1965; Avdeev et al., 1974).

Proterozoic stratified rocks in the western part of the Aktau–Mointy Massif are characterized by the higher degree of structural-metamorphic reworling as compared to its eastern part and are usually ascribed to the Upper Atasu Group, which includes (from bottom upward): Urkendeu Formation of felsic volcanic rocks, Kabantau and Aidarkharly formations consisting of quartzite schists, quartzites, and felsic volcanic rocks. The Urkendeu Formation (1000 m thick) is formed by felsic porphyroids with horizons of brecciated quartzites and quartzite schists thinning out along strike. The Kabantau Formation (300 m thick) comprises schists and quartzites in its lower part (400 m thick) and alternation of thick units of felsic porphyroids and quartzites in the upper part. The Aidarkharly Formation (300 m thick) is represented by alternation of felsic porphyroids and quartzites (Zaitsev et al., 1980).

Thus, the pre-Vendian stratified complexes in the western and eastern parts of the Aktau–Mointy Massif sharply differ in structure of their sequences and the degree of structural-metamorphic transformation. In the eastern part, the felsic volcanogenic sequences occupy the highest structural position, overlying the quartzite–schist units. In the western part of the massif, the felsic volcanic rocks are observed at the several structural levels, which are separated by quartzite–schist units. This explains the existence of two alternative stratigraphic schemes of the Pre-Vendian basement of the Aktau–Mointy Massif. According to the first scheme, the basement includes a single Late Riphean felsic volcanogenic sequence, while its different structural position in different parts of the massif is related to the later tectonic reworking (Avdeev et al., 1974; Avdeev and Kovalev, 1989). Large flat-lying and recumbent folds deformed by imbricated thrusts are inferred in the western part of the massif. This explains the lowest structural position of felsic volcanic sequence and repeated alternation of porphyroids and quartz–schist sequences. An alternative scheme suggests distinguishing several volcanogenic sequences at different structural levels of the basement, which were formed over almost entire Proterozoic (Zaitsev et al., 1980).

Felsic volcanic sequences that occupy different structural position in the sections of the eastern and western parts of the Aktau–Mointy Massif basement are similar in composition. They are represented by coarsely and finely fluidal rhyolites and subalkaline rhyolites. Phenocrysts are mainly represented by quartz and perthitic orthoclase, with subordinate plagioclase (<5–10%). The total content of phenocrysts in the rocks varies from 20 to 35%. The groundmass of the volcanic rocks is made up of micro- and fine-grained quartz–feldspathic aggregate.

In addition to the stratified rocks, the basement of the Aktau–Mointy Massif includes granite intrusions of the Uzunzhal Complex (Avdeev et al., 1990; *Geologicheskaya karta*..., 1981) cutting across the quartzite–schist sequences and felsic volcanics. The largest granite intrusions of this complex in the eastern part of the massif are the Shumek and Uzunzhal plutons (Fig. 1), which practically were not subjected to structural-metamorphic modifications. They consist mainly of massive coarse-grained to giant porphyritic biotite granites of the main phase. The rocks of the younger phase are represented by fine to medium-grained leucogranites developed in subordinate amount (<5% vol %). In the western part of the Aktau–Mointy Massif, the granites of the Uzunzhal Complex compose the Zhamantas, and the Northern

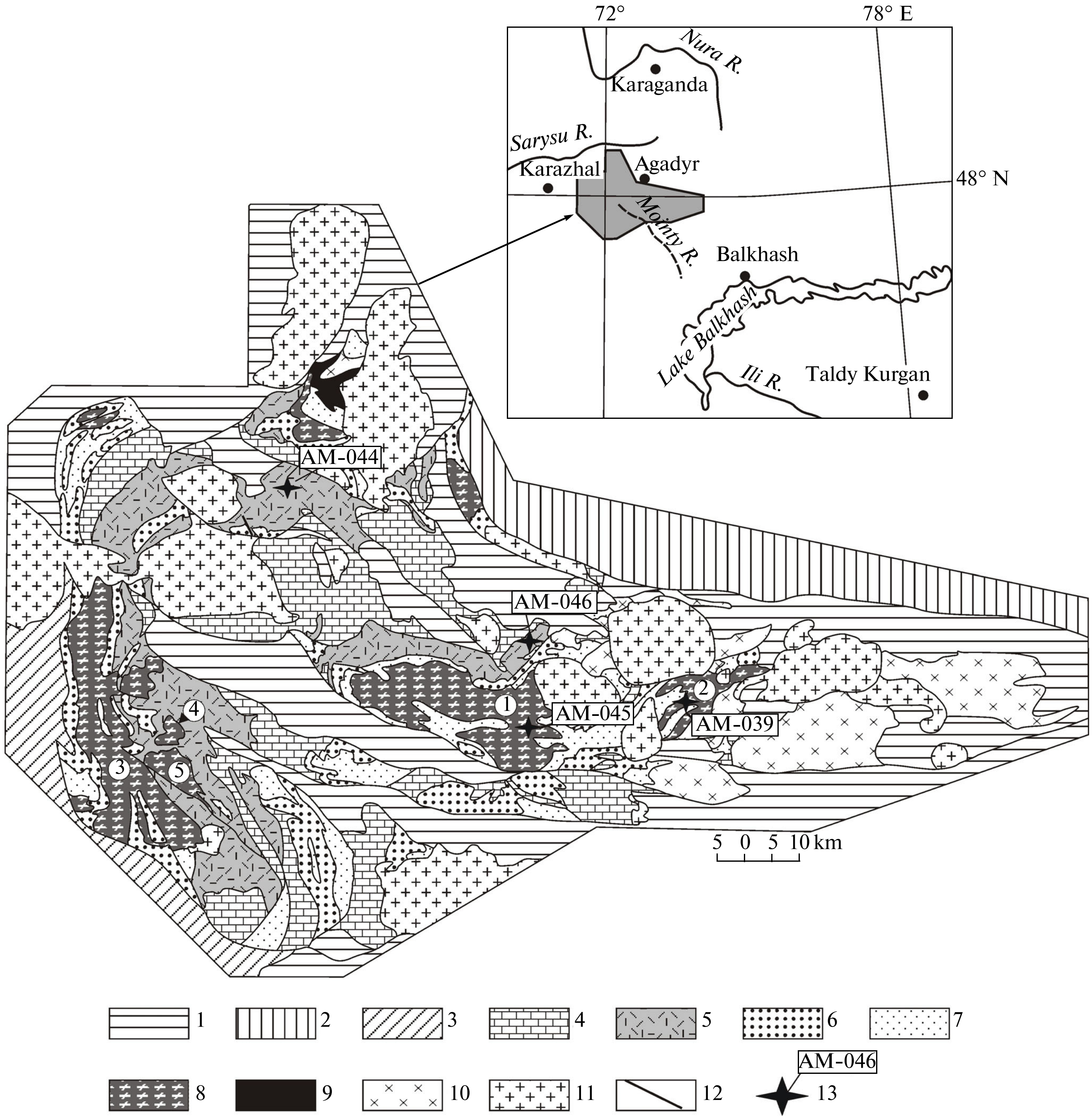

Fig. 1. Geological scheme of the Aktu–Mointy sialic massif. (1) Middle–Upper Paleozoic terrigenous–volcanogenic complexes; (2) Ordovician–Silurian siliceous–basaltic and terrigenous complexes; (3) Lower Paleozoic siliceous and terrigenous complexes; (4) Vendian–Lower Paleozoic terrigenous–carbonate cover of the Aktau–Mointy sialic massif; (5–8) basement complexes of the massif: (5) Neoproterozoic metamorphosed felsic volcanic rocks, (6) quartzites, (7) schists, (8) Neoproterozoic granitoids of the Uzunzhal Complex; (9) ophiolites; (10) Early Paleozoic granodiorites and monzonites; (11) Middle–Late Paleozoic granitoids; (12) faults; (13) sampling localities for U–Pb geochronological studies and their numbers. Numbers in circles show the granite plutons of the Uzunzhal Complex: (1) Uzunzhal, (2) Shumek, (3) Zhamantas, (4) Northern Kabantau, (5) Southern Kabantau massifs.

and Southern Kabantau plutons (Fig. 1). We studied the rocks of the Southern Kabantau Pluton, which was described in detail for the first time by German and Filippovich (1987). Unlike the granites of the Uzunzhal Complex in the eastern part of the Aktau–Mointy Massif, the granites of this pluton are strongly sheared and locally transformed into augen blastomylonites. Its contacts with host rocks are usually tectonic.

It is noteworthy that the stratified basement complexes and the Uzunzhal granites within the western part of the Aktau–Mointy Massif experienced intense structural-metamorphic evolution. This suggests that the section of the Proterozoic stratified complexes in this part of the massif is disturbed and corresponds to the inverse stratigraphic succession.

ANALYTICAL

The major element composition of the rocks was analyzed by XRF method at the GIN RAS (Moscow) on a sequential S4 Pioneer Bruker spectrometer using Spectra-Plus software, while the trace element composition was studied by ICP-MS with relative error no more than 10% at the Institute of Mineralogy, Geochemistry, and Crystallochemistry of Rare Elements, Ministry of Natural Resources of the Russian Federation, Moscow.

U–Pb geochronological studies were carried out at the IPGG RAS (St. Petersburg). Accessory zircons were extracted using a heavy-liquid conventional technique. Zircon crystals selected for U–Pb geochronological study were subjected to a multistage removal of surface contamination by alcohol, acetone, and 1 M HNO_3. After each stage, zircon grains were rinsed in ultrapure water. The chemical decomposition of zircon and extraction of U and Pb were performed using a modified Krogh technique (Krogh, 1972). Air-abrasion (Krogh, 1982) and preliminary acid treatment (Mattinson, 1994) were sometimes applied to decrease the discordance degree. Isotope studies were carried out using ^{235}U–^{202}Pb and ^{235}U–^{208}Pb mixed isotope tracers. Isotope analyses were made on a Finnigan MAT-261 multicollector mass spectrometer in static and dynamic (using electron multiplier) modes. The contents of U and Pb, as well as U/Pb isotope ratios were determined accurate to 0.5%. The procedure blanks were less than 15 pg Pb and 1 pg U. Experimental data were processed using PbDAT (Ludwig, 1991) and ISOPLOT (Ludwig, 1999) programs. The ages were calculated using conventional uranium decay constants (Steiger and Jager, 1976). Corrections for common lead were introduced in compliance with model values (Stacey and Kramers, 1975). All errors are given at 2σ level.

Sm–Nd isotope geochemical studies were carried out at the IGEM RAS (Moscow). Sm and Nd were extracted using technique (Larionova et al., 2007). The Sm and Nd isotope compositions were analyzed on a Sector-54 multicollector spectrometer in a dynamic mode on a triple-filament ion source (Thirlwall, 1991). Measured ^{143}Nd/^{144}Nd ratios were normalized to ^{146}Nd/^{144}Nd = 0.7219 and reduced to ^{143}Nd/^{144}Nd = 0.511860 in the La Jolla Nd standard. The ^{149}Sm–^{150}Nd tracer used in our studies was added to sample aliquots (0.2–0.3 g) before chemical decomposition. The measurement accuracies were ±0.5% for Sm and Nd, ±0.2% for ^{147}Sm/^{144}Nd ratio, and ±0.002% for ^{143}Nd/^{144}Nd (2σ). Blanks were less than 15 pg for Sm and 50 pg for Nd.

RESULTS OF THE U–Pb GEOCHRONOLOGICAL STUDIES

To determine the age of the Proterozoic igneous rocks of the Aktau–Mointy Massif, U–Pb geochronological studies were performed for felsic volcanic rocks of the Altyn Syngan and Urkendeu formations as well as for the Uzunzhal granitois cutting across them.

The Altyn Syngan Formation. Accessory zircon extracted from weakly metamorphosed porphyritic trachyrhyolite of the Altyn Syngan Formation (sample AM-046, 47°45′13.20″ N; 72°49′12.40″ E) forms subeuhedral and euhedral transparent and semitransparent brown crystals of short-to long-prismatic habit. The crystals are shaped by {100} and {110} prisms and {122}, {111}, and {101} bipyramids (Fig. 2, I–III). They show weakly expressed magmatic zoning; fragments of zoning were also identified in the irregularly shaped core relicts in semitransparent crystals (Fig. 2, IV–VI). The crystal size varies from 40 to 100 μm, K_{el} = 2.2–4.0.

Four microaliquots of transparent zircon grains taken from size fraction > 85 μm and 85 + 53 μm (Table 1, nos. 1–4) were used for U–Pb geochronological study. Two of these microaliquots were subjected to preliminary air abrasion (Table 1, nos. 3–4). As seen from Fig. 3, the data points of untreated zircon (Table 1, nos. 1, 2) and zircon after removal of 20% of its material (Table 1, no. 4) define regression with an upper-intercept age of 925 ± 9 Ma (MSWD = 011) and the lower-intercept age of 281 ± 38 Ma. Somewhat older age (^{207}Pb/^{206}Pb) was determined in zircon subjected to more pervasive (40%) air abrasion (Table 1, no. 3), which is presumably related to the presence of inherited radiogenic lead component. Since the morphology of the studied zircon indicates its magmatic origin, the age of 925 ± 9 Ma may be interpreted as the crystallization age of parental melts of the felsic volcanic rocks of the Altyn Syngan Formation.

Urkendeu Formation. Accessory zircon from porphyritic rhyodacites of the Urkendeu Formation (sample AM-044; 47°58′52.50″ N; 72°16′14.58″ E) is represented by subeuhedral semitransparent and transparent brown and yellow-brown crystals of short- and long-prismatic habit. The crystals are shaped by {100} and {110} prisms and {111}, {101}, and {112} bipyramids (Fig. 4, I–IV). They usually show magmatic zoning (Fig. 4, V–VIII). Some of them contain both crystalline and metamict fractured cores with diffuse borders (Fig. 4, VII). Crystal size is 40–200 μm, K_{el} = 2.0–4.0.

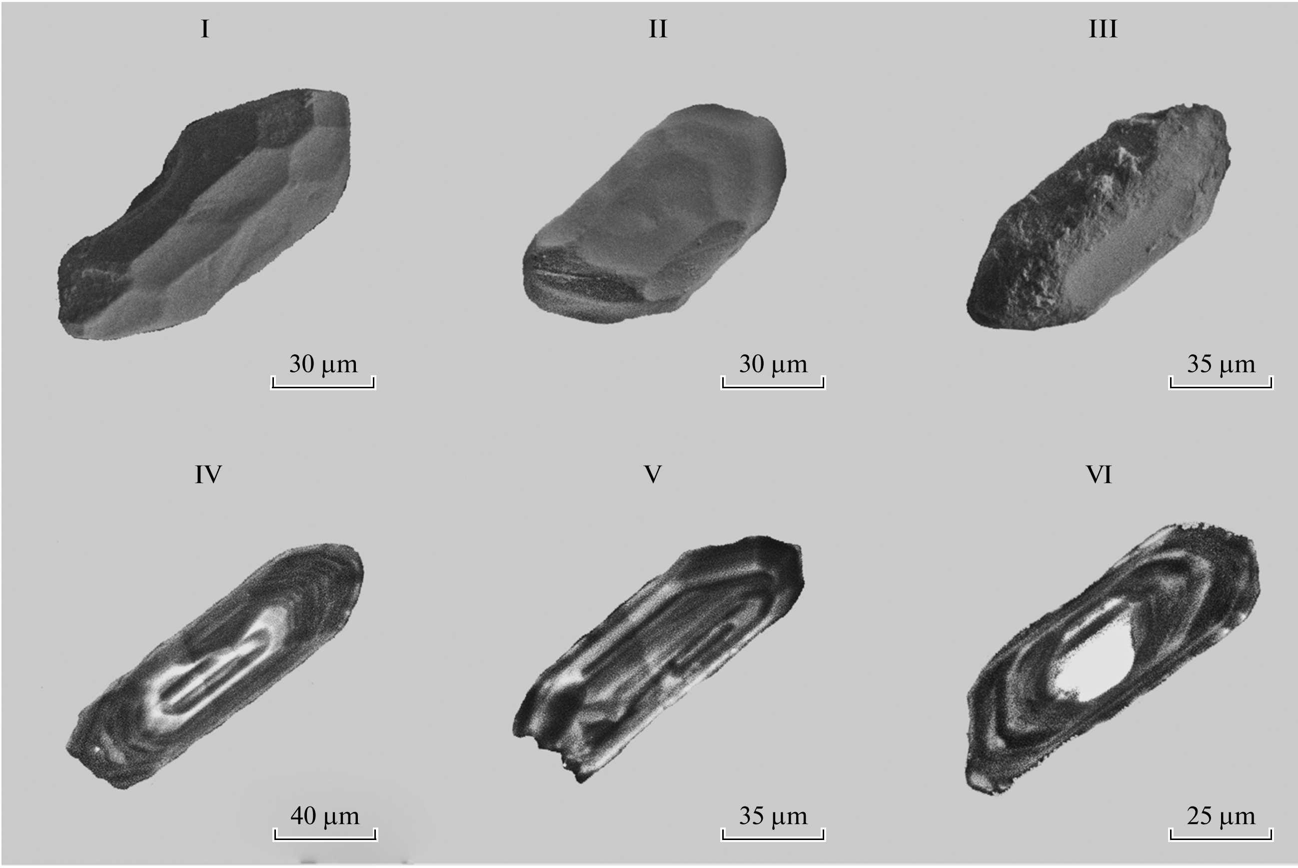

Fig. 2. Microimages of zircon crystals from the porphyritic trachyrhyolite of the Altyn Syngan Formation (sample AM-046) made using an ABT 55 scanning electron microscope. (I–III) secondary electron regime; (IV–VI) cathodoluminescence regime.

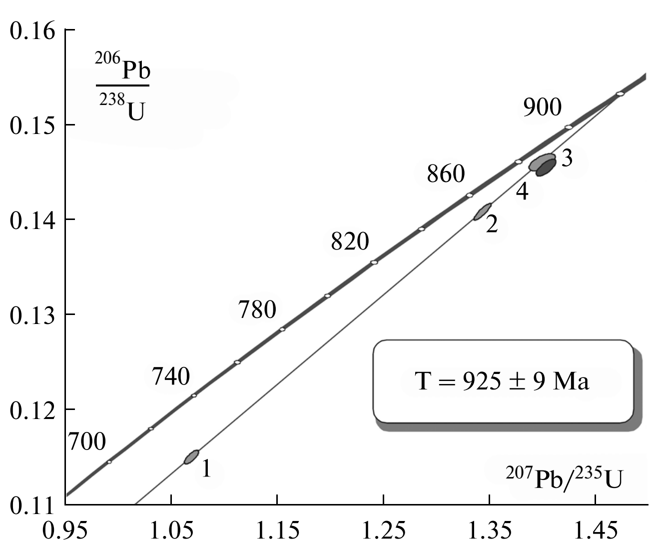

Fig. 3. Concordia diagram for zircons from weakly metamorphosed porphyritic subalkaline rhyolites of the Altyn Syngan Formation (sample AM-046). Numbers of data points in the diagram correspond to those in Table 1.

Five microaliquots (10–50 grains) of the most transparent zircon crystals collected from size fractions >100, –100 + 85, and –85 + 53 μm (Table 1, nos. 5–9) were selected for U–Pb geochronological study. Three of them (Table 1, nos. 5, 6, 9) are characterized by the least discordant age values. Their data points define a discordia (Fig. 5) with an upper-intercept age of 942 ± 67 Ma and almost zero lower intercept (MSWD = 0.43). The data points of two more microaliquots of zircon (Fig. 5, Table 1, nos. 7, 8) lie to the right of discordia, showing the presence of older inherited cores in them. Significant error in age of zircon from the porphyritic rhyodacites of the Urkendeu Formation is related to the sufficiently compact distribution of data points around the upper intercept of discordia. Therefore, the average age calculated from $^{207}Pb/^{206}Pb$ ratio for zircons, the data points of which fit the discordia (Fig. 5, Table 1, nos. 5, 6, 9), is regarded as the most accurate estimation of the crystallization age of the studied zircons, and, correspondingly, as the formation age of the volcanic rocks of the indicated formation. This is 921 ± 5 Ma (MSWD = 1.5) and coincides within error with the upper-intercept age.

Table 1. Results of U–Pb geochronological study of accessory zircons from the Neoproterozoic volcanic rocks of the Altyn Syngan and Urkendeu formations and granites of the Uzunzhal Complex of the Aktau–Mointy sialic massif

Ordinal no.	Size fraction (μm) and characteristics	Weight, mg	Pb, ppm	U, ppm	Isotope ratios					Rho	Age, Ma		
					$^{206}Pb/^{204}Pb$	$^{207}Pb/^{206}Pb^a$	$^{208}Pb/^{206}Pb^a$	$^{207}Pb/^{235}U$	$^{206}Pb/^{238}U$		$^{207}Pb/^{235}U$	$^{206}Pb/^{238}U$	$^{207}Pb/^{206}Pb$
Porphyritic subalkaline rhyolite of the Altyn Syngan Formation (sample AM-046)													
1	>85	0.05	25.7	210	634	0.0692 ± 1	0.0935 ± 1	1.0703 ± 26	0.1122 ± 2	0.77	739 ± 2	685 ± 1	905 ± 3
2	50–85	–*	U/Pb = 6.1		366	0.0693 ± 2	0.1336 ± 1	1.3469 ± 77	0.1409 ± 7	0.80	866 ± 5	850 ± 4	908 ± 7
3	50–85, A = 40%	–*	U/Pb = 6.6		758	0.0700 ± 3	0.1068 ± 1	1.4046 ± 76	0.1456 ± 6	0.71	891 ± 5	876 ± 4	927 ± 8
4	50–85, A = 20%	–*	U/Pb = 6.5		375	0.0695 ± 4	0.0653 ± 1	1.4013 ± 101	0.1462 ± 7	0.63	889 ± 6	880 ± 4	914 ± 12
Porphyritic rhyodacite of the Urkendeu Formation (sample AM-044)													
5	>100	–*	U/Pb = 5.8		287	0.0697 ± 4	0.1020 ± 2	1.4312 ± 100	0.1490 ± 6	0.48	903 ± 6	895 ± 4	918 ± 13
6	50–85	0.09	43.1	289	1394	0.0695 ± 2	0.0852 ± 1	1.4344 ± 43	0.1496 ± 3	0.52	903 ± 3	899 ± 2	915 ± 5
7	85–100	0.14	61.8	404	3181	0.0722 ± 1	0.0848 ± 1	1.5133 ± 30	0.1521 ± 3	0.89	936 ± 2	913 ± 2	991 ± 1
8	>100	0.12	84.2	547	3500	0.0707 ± 1	0.0911 ± 1	1.4878 ± 30	0.1525 ± 3	0.90	925 ± 2	915 ± 2	950 ± 1
9	>100	0.07	82.7	538	1796	0.0699 ± 1	0.0812 ± 1	1.4616 ± 29	0.1517 ± 3	0.78	915 ± 2	911 ± 2	925 ± 2
Biotite granite of the Shumek Pluton (sample AM-039)													
10	>100, A = 50%	–*	U/Pb = 7.0		4619	0.0698 ± 1	0.0574 ± 1	1.4009 ± 47	0.1456 ± 4	0.82	889 ± 3	876 ± 2	922 ± 4
11	85–100, A = 40%	–*	U/Pb = 6.9		3669	0.0698 ± 2	0.0583 ± 2	1.4346 ± 59	0.1490 ± 4	0.72	903 ± 4	895 ± 3	923 ± 6
12	85–100, A = 50%	–*	U/Pb = 6.8		2892	0.0696 ± 1	0.0672 ± 1	1.4467 ± 48	0.1507 ± 4	0.88	908 ± 3	905 ± 3	917 ± 3
Biotite granite of the Uzunzhal Pluton (sample AM-045)													
13	50–85	–*	U/Pb = 6.8		2234	0.0696 ± 1	0.0898 ± 1	1.3872 ± 28	0.1444 ± 3	0.94	884 ± 2	870 ± 2	918 ± 1
14	50–85, A = 40%	0.05	31.1	214	961	0.0703 ± 2	0.1348 ± 1	1.3357 ± 59	0.1379 ± 5	0.70	861 ± 4	833 ± 3	936 ± 7
15	>85, A = 30%	–*	U/Pb = 6.3		976	0.0698 ± 2	0.1475 ± 1	1.4305 ± 66	0.1486 ± 5	0.62	902 ± 4	893 ± 3	923 ± 8
16	>85, acid tr. = 3.0	–*	U/Pb = 5.9		1174	0.0702 ± 1	0.1837 ± 1	1.4642 ± 33	0.1512 ± 3	0.67	916 ± 2	908 ± 2	935 ± 3
17	<85, A = 20%	–*	U/Pb = 5.5		321	0.0730 ± 2	0.1174 ± 1	1.5380 ± 66	0.1529 ± 5	0.65	946 ± 4	917 ± 3	1013 ± 7

* Isotope ratios corrected for blank and common lead; Rho is the coefficient of $^{207}Pb/^{235}U$–$^{206}Pb/^{238}U$ correlation; A = 20% is the amount of zircon removed during air abrasion treatment; *weight of zircon was not determined; ac. tr. = 3.0 is the zircon residue after acid treatment for 3 hours. Errors (2SD) correspond to the last significant digits.

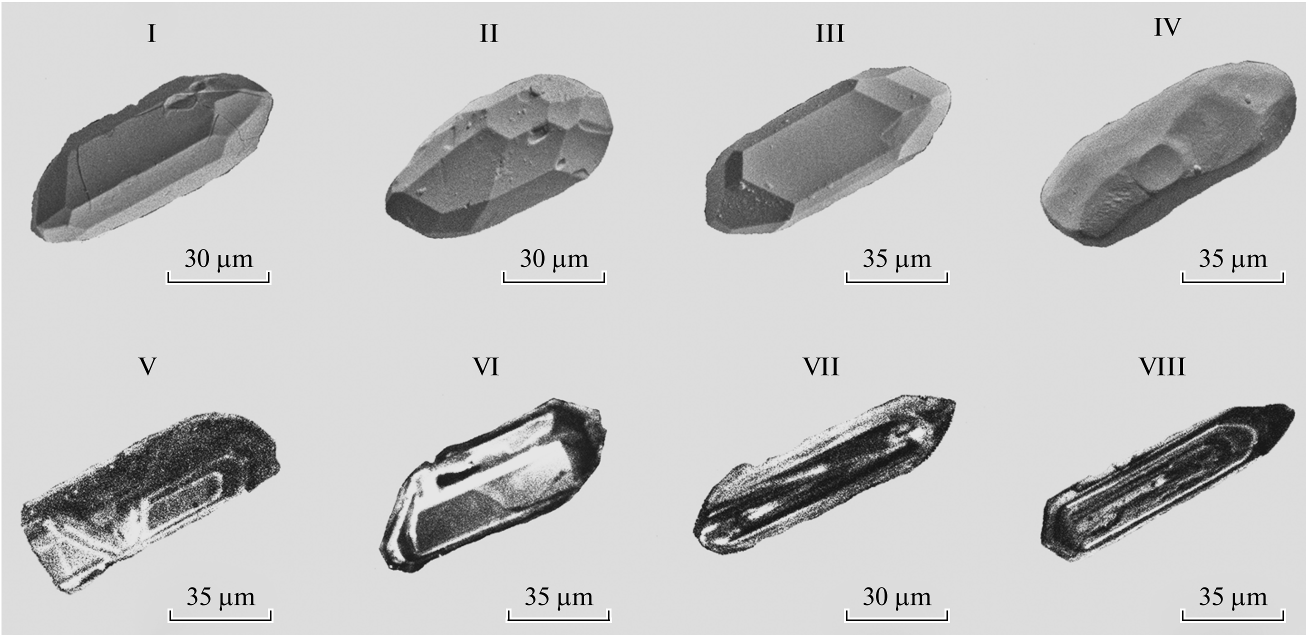

Fig. 4. Microimages of zircon crystals from the porphyritic rhyodacites of the Urkendeu Formation (sample AM-044) made on an ABT 55 scanning electron microscope. (I–IV) secondary electron regime, (V–VIII) catodoluminescence regime.

Shumek Pluton. Zircons extracted from the biotite granites of the Shumek Pluton (sample AM-039; 47°38′37.68″ N; 73°11′34.98″ E) are transparent and semitransparent euhedral and subeuhedral light brown and brown-pinkish crystals of prismatic, short-prismatic (Fig. 6, I–III), and acicular shapes. The crystals show a combination of {100} and {110} prisms and {101}, {111}, and {112} bipyramids (Fig. 6, 1–III). They have poorly expressed zoned structure (Fig. 6, IV–VI). In the outer parts of many crystals, zoning is partially disturbed by formation of "sugar" like shell with lowered birefringence. The majority of the crystals contain assimilated cores of irregular shape with diffuse borders (Fig. 6, IV–VI), which are enriched in dust-like and solid-phase mineral inclusions. The crystal size varies from 50 to 150 μm, K_{el} = 2.0–3.3.

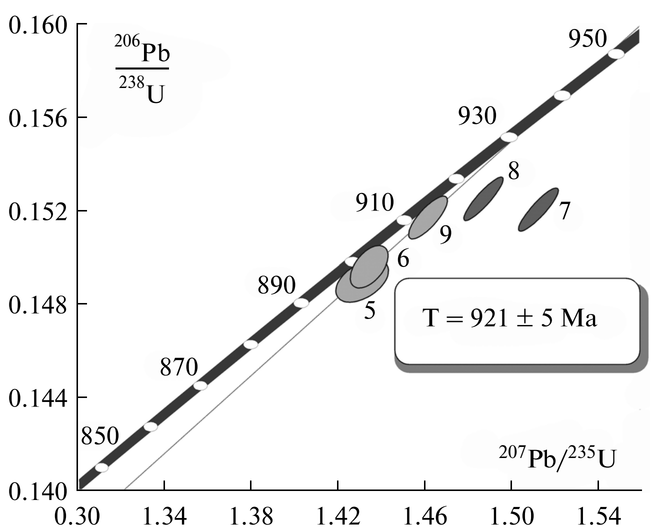

Fig. 5. Concordia diagram for zircon from the porphyritic rhyodacites of the Urkendeu Formation (sample AM-044). Numbers of data points in the diagram correspond to the ordinal numbers in Table 1.

Three zircon microaliquots from size fractions >100 μm and –100 + 85 μm subjected to preliminary air abrasion (Table 1, nos. 10–12) were used for U–Pb dating. Data points of these microaliquots define discordia (Fig. 7) with the upper-intercept age of 917 ± 6 Ma and the lower-intercept age of –198 ± 340 Ma (MSWD = 1.1). Morphology of this zircon points to its crystallization from a melt. Hence, the age of 917 ± 6 Ma may be regarded as the emplacement age of the Shumek Pluton.

Uzunzhal Pluton. Accessory zircon from biotite granite of the Uzunzhal Pluton (sample AM-045; 47°41′27.60″ N; 72°16′14.58″ E) is represented by euhedral and subeuhedral transparent and semitransparent brownish prismatic and short-prismatic crystals, which are shaped by {100} and {110} prisms and {111}, {101} dipyramids (Fig. 8. I–III). Their inner structure is determined by "thin" and sectorial zoning (Fig. 8, IV–VI). Some crystals contain relicts of crystalline and metamictic cores of prsimatic and oval shape with blurred margins (Fig. 8, IV–VI), as well as

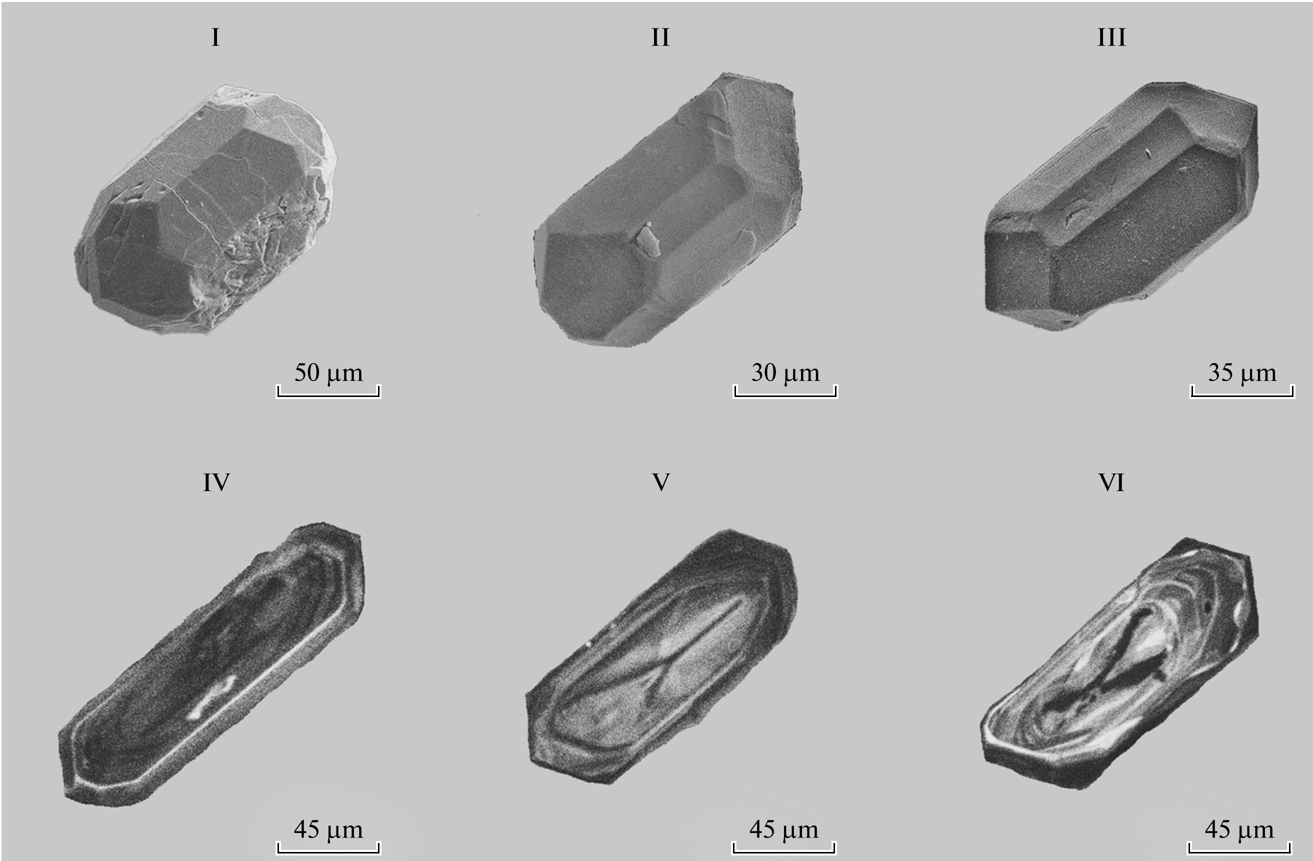

Fig. 6. Microimages of zircon crystals from the biotite granite of the Shumek Pluton (sample AM-039) made on an ABT 55 scanning electron microscope: (I–III) secondary electron image; (IV–VI) cathodoluminescence image.

rims with lowered birefringence. Crystal size is 40–100 μm, K_{el} = 2.0–2.2.

Five microaliquots of the most transparent and euhedral zircons collected from size fractions >85 μm, −85+53 μm, and < 85 μm (Table 1, nos. 13–17) were taken for U–Pb dating. Three microaliquots were subjected to the preliminary air abrasion treatment (Table 1, nos. 14, 15, 17), and one microaliquot was subjected to the preliminary acid treatment (Table 1, no. 16). Data points of microaliquots of untreated zircon (Table 1, no. 13) and air-abraded and acid treated microaliquots of zircon from fraction > 85 μm define a discordia (Fig. 9) with the upper-intercept age of 945 ± 22 Ma and the lower-intercept age of 373 ± 190 Ma (MSWD = 0.95). Data points of air-abraded zircons from fractions −85 ± 53 μm and <85 μm plot to the right of concordia, which indicates the presence of small amount of inherited radiogenic lead. The morphological features of the studied zircon indicate its magmatic origin. Hence, age value of 945 ± 22 Ma corresponds to the formation age of the Uzunzhal Pluton.

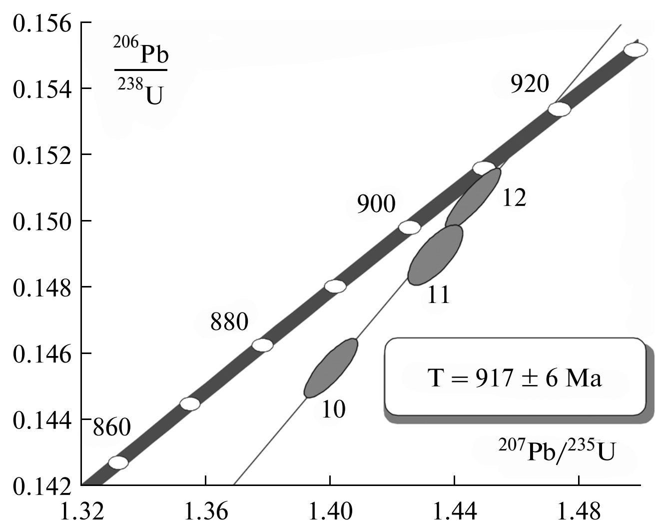

Fig. 7. Concordia diagram for zircons from the biotite granite of the Shumek Pluton (sample AM-039). Numbers of data points correspond to the ordinal numbers in Table 1.

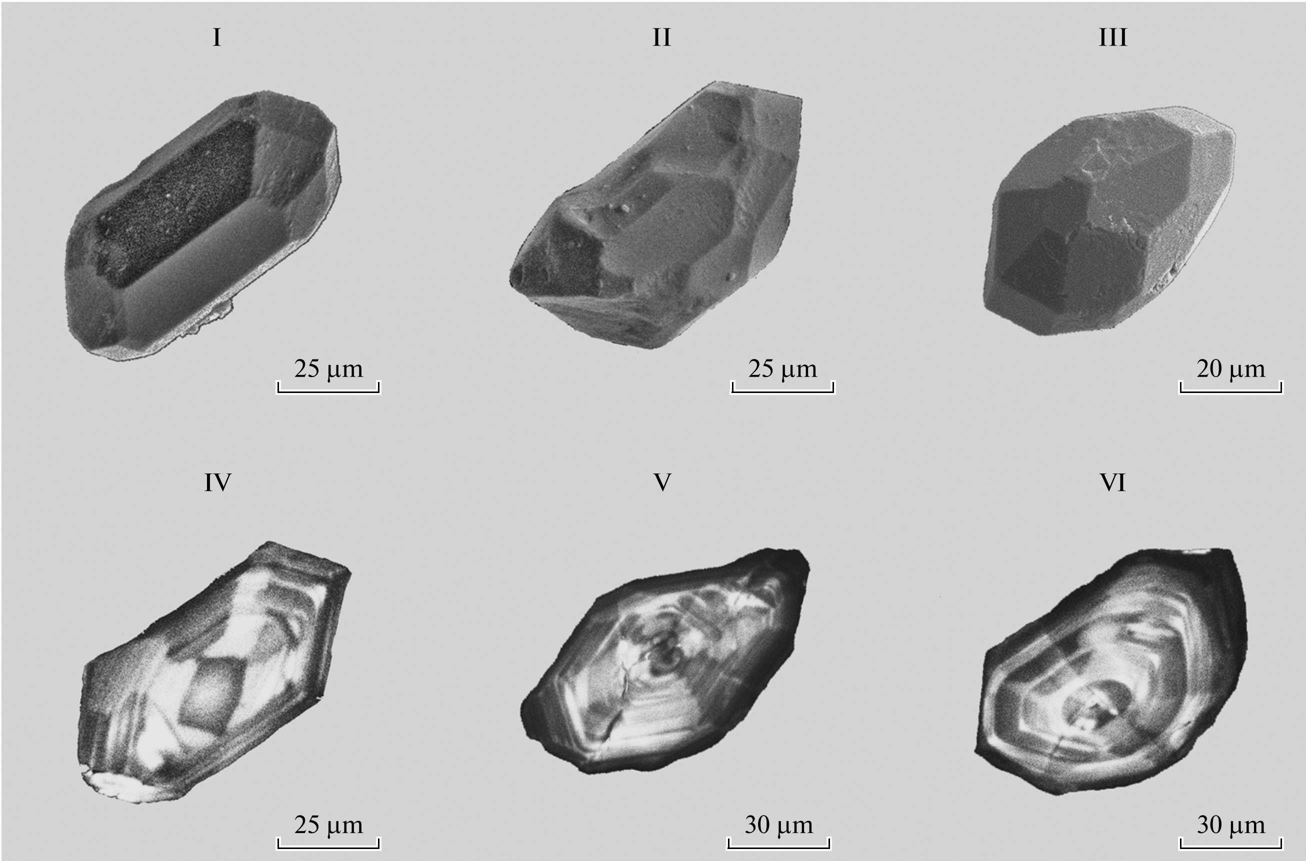

Fig. 8. Microimages of zircon crystals from the biotite granite of the Uzunzhal Pluton (sample AM-045) made on an ABT 55 scanning electron microscope: (I–III) secondary electron regime, (IV–VI) cathodoluminescence regime.

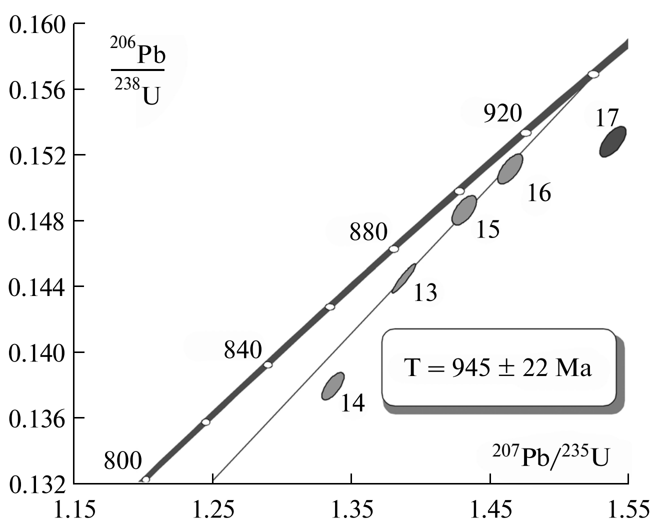

Fig. 9. Concordia diagram for zircons from biotite granite of the Uzunshal Pluton (sample AM-045). Data points in the diagram correspond to the ordinal numbers in Table 1.

GEOCHEMISTRY OF THE VOLCANIC ROCKS AND GRANITES

To characterize the composition of the Neoproterozoic igneous rocks of the Aktau–Mointy Massif basement, we analyzed the contents of major and trace elements (Tables 2, 3) in the least altered volcanic rocks of the Altyn Syngan (eastern part) and Urkendeu (western part) formations and cross-cutting granites of the Uzunzhal Complex.

In terms of the major-element composition, the volcanic rocks of the Altyn Syngan Formation correspond to rhyodacites, rhyolites, and trachyrhyolites (SiO_2 68–76 wt %, $\Sigma Na_2O + K_2O$ 7.0–8.7 wt %) of high-K calc-alkaline series (K_2O/Na_2O 2.3–6.2), while the porphyritic biotite granites and leucocratic granites of the Uzunzhal Complex are ascribed, respectively, to granites and subalkaline granites (SiO_2 71–73 wt %, $\Sigma Na_2O + K_2O$ 7.0–8.2 wt %), and leucogranites (SiO_2 73–74 wt %, $\Sigma Na_2O + K_2O$ 7.8–8.2 wt %). The albitized varieties of the porphyritic biotite granites of the Shumek Pluton differ in the significant predominance of Na_2O over K_2O (K_2O/Na_2O – 0.2).

In general, the volcanic rocks of the Altyn Syngan Formation are chemically close to the granites of

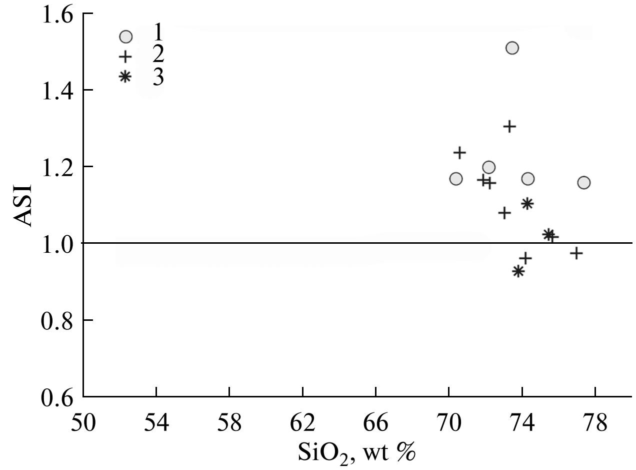

Fig. 10. Diagram ASI (Al/(Ca – 1.67P + Na + K))–SiO_2 for the Neoproterozoic magmatic rocks of the Aktau–Mointy sialic massif. (1) Felsic volcanic rocks of the Altyn Syngan Formation; (2) granites of the Uzunzhal Pluton; (3) granites of the Shumek Pluton. Lines separate the peraluminous and metaluminous rocks (Frost C.D., Frost, B.R., 2011).

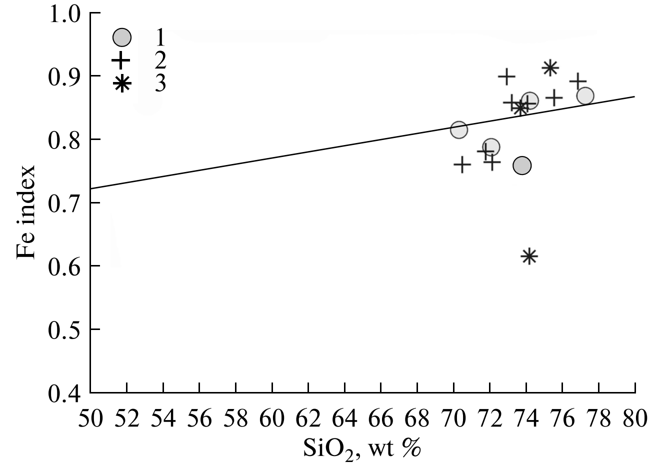

Fig. 11. Diagram Fe index (FeO + $0.9Fe_2O_3$)/(FeO + $0.9Fe_2O_3$ + MgO)–SiO_2 for the Neoproterozoic magmatic rocks of the Aktau–Mointy sialic massif. Symbols are shown in Fig. 10. Lines separate the fields of ferroan and magnesian granitoids (Frost, C.D., Frost, B.R., 2011).

Uzunzhal Complex, which is expressed in their affiliation to peraluminous rocks (ASI_{volc} = 1.17–1.5; ASI_{gran} = 0.93–1.2) of high-K calc-alkaline (K_2O/Na_2O_{volc} 2.7–6.1; K_2O/Na_2O_{gran} = 1–2.18), and ferroan $(FeO^*/(FeO + MgO)_{volc} = 0.75–0.87$; $FeO^*/(FeO + MgO)_{gr} = 0.62–0.92$) series (Figs. 10, 11). In addition, they show similar REE distribution (Fig. 12) with LREE enrichment ($(La/Yb)_n = 4.3–7.2$ in the volcanic rocks and 4.4–9.5 in the granites) and the well pronounced negative Eu anomaly (Eu/Eu*= 0.2–0.4 in the volcanic rocks and 0.23–0.35 in granites). In the multielement diagrams (Fig. 13), the considered volcanic rocks and granites exhibit sharply expressed negative Ti, Sr, P, and Eu anomalies, the least expressed negative Nb, Ta, and Ba anomalies and the positive Cs, Rb, Th, and U anomalies.

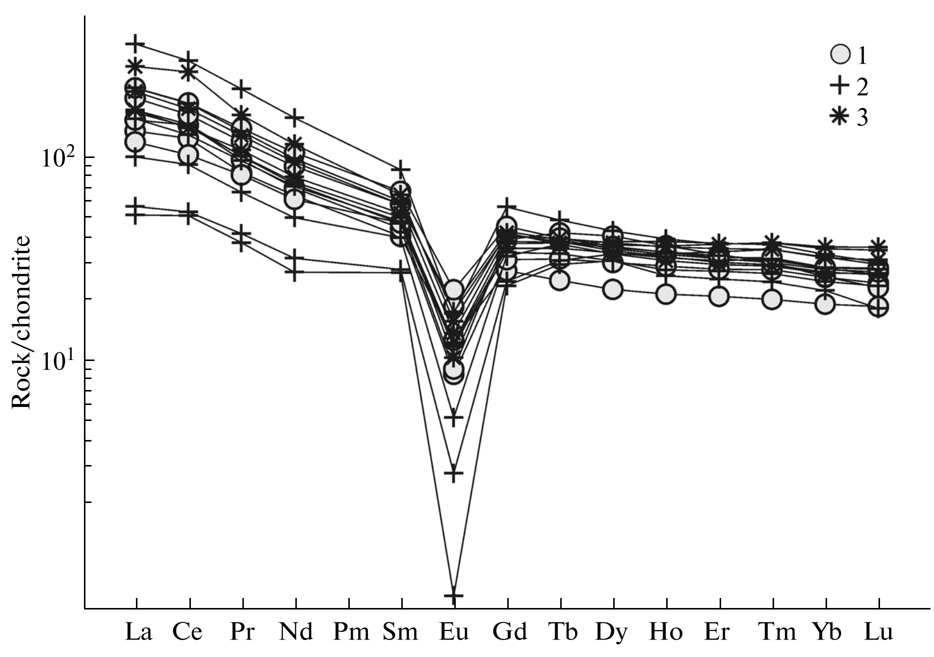

Fig. 12. REE distribution in the Neoproterozoic magmatic rocks of the Aktau–Mointy sialic massif. Symbols are shown in Fig. 10. REE contents are normalized to chondrite composition (Sun and McDonough, 1989).

Table 2. Content of major (wt %) and trace (ppm) elements in the Late Precambrian volcanic rocks of the Altyn Syngan and Urkendeu formations and in the granitoids of the Uzunzhal Complex

Component	Volcanic rocks of the Altyn Syngan and Urkendeu formations					Granitoids of the Uzunzhal Complex		
	1	2	3	4	5	6	7	8
	AM005-1	AM007	AM008	AM009	AM044	AM139	AM141-1	AM142
SiO_2	70.56	73.24	75.80	71.20	67.88	71.82	70.53	72.18
TiO_2	0.39	0.30	0.19	0.36	0.47	0.251	0.35	0.30
Al_2O_3	13.53	13.02	11.28	13.40	14.41	13.97	14.65	13.83
Fe_2O_3	3.37	2.25	2.00	3.33	1.67	0.6	0.70	1.04
FeO	0.22	0.56	0.36	0.43	2.23	1.57	1.89	1.31
MnO	0.02	0.02	0.01	0.02	0.05	0.024	0.03	0.03
MgO	0.87	0.41	0.32	1.17	0.85	0.586	0.79	0.69
CaO	0.35	0.30	0.45	0.35	1.88	0.998	0.79	0.99
Na_2O	2.15	2.31	1.08	1.30	2.15	2.386	2.72	2.59
K_2O	6.58	6.28	6.62	5.64	4.95	5.747	5.48	5.43
P_2O_5	0.13	0.16	0.12	0.14	0.14	0.098	0.11	0.10
LOI	1.80	1.35	1.80	2.54	2.40	1.78	1.76	1.31
Total	99.97	100.20	100.03	99.88	99.08	99.83	99.79	99.80
Sc	5.44	5.41	3.21	7.13	3.07	1.3	18.09	4.48
Ti	2109	1695	969	1914	2346	3432	2025.7	2427
V	27	19.3	10.7	24.3	28.1	26.8	21.69	19.65
Cr	15.2	14.9	6.2	14.6	21	42.04	27.59	79.97
Rb	252	385	389	282	228.5	299.8	263.52	228.8
Sr	33	46	34	32	96	66.91	62.87	64.45
Y	35	49.1	66.8	56.6	56.1	57.41	45.43	42.7
Zr	153	195	117	151	268	537.5	220.43	158.6
Nb	10.4	10.98	10.19	10.49	12.04	18.82	9.94	10.93
Cs	16.81	23.27	11.68	14.89	6.01	10.78	4.53	3.47
Ba	673.6	329.6	226.5	571.2	912	548.4	636.21	497.6
La	31.2	35.4	27.6	45.3	50.9	83.67	50.79	39.56
Ce	74.3	86.3	61.6	97.1	111	178.7	110.2	86.86
Pr	7.84	9.03	7.63	11.11	12.9	20.13	12.49	9.41
Nd	29.7	32.3	28.4	41.3	48.2	71.42	45.03	33.71
Sm	6.12	6.71	7.13	8.8	10.2	13.02	9.11	7.1
Eu	0.72	0.49	0.52	1.05	1.27	0.97	0.99	0.67
Gd	5.58	6.32	7.92	8.69	9.22	11.48	8.39	6.86
Tb	0.91	1.16	1.56	1.44	1.47	1.8	1.41	1.23
Dy	5.58	7.57	10.2	8.83	9.08	10.82	8.66	7.7
Ho	1.18	1.62	2.04	1.85	1.89	2.2	1.8	1.55
Er	3.36	4.56	5.39	5.15	5.21	6.07	4.94	4.47
Tm	0.5	0.7	0.76	0.76	0.8	0.95	0.74	0.67
Yb	3.16	4.28	4.31	4.68	4.79	5.92	4.54	4.08
Lu	0.46	0.6	0.57	0.68	0.71	0.87	0.66	0.58
Hf	4.62	5.99	3.96	4.66	7.09	14.82	6.81	4.6
Ta	0.94	1.15	1.18	0.98	1	1.55	1.04	1.05
Pb	24.5	30.9	16.1	8.8	32.2	29.52	31.06	21.15
Th	17.27	27.38	20.48	23.36	29.1	67.54	35.82	28.28
U	3.18	3.24	4.01	3.04	3.73	6.49	3.85	3.36

Table 2. (Contd.)

Granitoids of the Uzunzhal Complex							
9	10	11	12	13	14	15	16
AM-143	AM012	AM045	AM010	AM011	AM019	AM020	AM021
73.26	72.52	71.16	74.80	74.22	71.80	72.82	72.73
0.14	0.27	0.32	0.17	0.17	0.27	0.42	0.53
14.60	12.79	13.00	11.62	11.10	12.20	13.00	12.44
0.69	1.00	2.00	0.60	2.77	1.36	1.65	0.96
0.84	1.50	1.80	0.79	1.08	1.61	1.15	1.79
0.02	0.04	0.04	0.04	0.03	0.03	0.02	0.02
0.24	0.40	0.40	0.16	0.55	0.50	1.64	0.25
0.75	1.23	1.46	0.90	0.24	1.11	0.34	0.69
2.45	4.05	2.40	2.63	2.85	3.24	6.11	5.76
5.35	4.05	5.01	5.49	5.34	5.34	1.01	1.30
0.16	0.08	0.12	0.12	0.10	0.05	0.11	0.10
1.43	0.95	1.52	1.20	1.48	2.02	1.70	2.34
99.91	99.51	99.23	99.52	99.93	99.53.	99.97	100.24
2.69	4.86	3.43	3.34	4.12	6.91	8.61	9.76
1645.67	1327	1555	728	893	1210	2173	2688
6.22	16.4	17.1	9	12.7	15.5	28.7	28.4
22.46	15.2	16	8.9	15.2	10.2	24.4	22.9
429.7	347	362.8	362	369	299	44	47.7
13.54	48	57	17	21	75	57	85
42.6	60.4	55.3	57.4	69.5	64.2	66.1	53.6
80.12	155	188	92	107	173	198	250
14.52	9.91	11.04	10	8.71	13.43	13.99	16.95
6.79	14.11	12.25	5.32	7.65	6.84	0.69	0.46
33.66	481.7	447	81.1	125.2	367.8	62.5	174.7
12.08	38.5	35.9	13.3	23.3	39.6	48.8	64.8
30.98	84.6	77.2	32.3	55.2	83.4	103.8	157.3
3.54	9.45	8.95	3.92	6.26	10.1	11.9	15
12.47	34.6	32.9	14.6	23.1	36.6	43.3	53
4.06	7.58	7.26	4.21	6.03	7.94	8.81	9.79
0.04	0.7	0.69	0.16	0.3	0.59	0.78	0.89
4.7	7.76	7.18	4.94	6.57	7.59	8.28	8.55
1.09	1.4	1.31	1.14	1.37	1.39	1.46	1.37
7.71	8.95	8.44	8.33	9.59	9.24	9.46	8.35
1.45	1.9	1.78	1.86	2.14	2.03	2.01	1.72
4.09	5.33	5.03	5.56	6.12	6.06	5.77	4.82
0.61	0.78	0.79	0.88	0.93	0.95	0.88	0.73
3.69	4.74	4.77	5.38	5.55	6.04	5.34	4.48
0.45	0.66	0.7	0.74	0.76	0.9	0.78	0.67
2.96	4.72	5.35	3.32	3.52	5.34	5.75	6.97
2.11	1.19	1.19	1.41	1.11	1.51	1.35	1.36
10.69	36.5	22.3	25.2	21.1	32.8	7.8	6.4
18.35	26.11	25	13.88	18.67	23.44	24.74	33.55
4.83	3.3	3.64	5.33	3.03	3.42	2.29	2.19

(1–4) Volcanic rocks of the Altyn Syngan Formation: (1–2) subalkaline rhyolites; (3–4) rhyolites; (5) rhyodacite of the Urkendeu Formation; (6–16) granitoids of the Uzunzhal Complex: (6–13) granitoids of the Uzunzhal Pluton; (6–8) subalkaline granites, (9, 11–13) leucogranites; (10) granite; (14–16) granitoids of the Shumek Pluton: (14) subalkaline granite; (15, 16) albitized granites.

Table 3. Petrochemical and geochemical characteristics of the Late Precambrian volcanic rocks of the Altyn Syngan and Urkendeu formations and granitoids of the Uzunzhal Complex

Component	1	2	3	4	5	6	7	8	9	10	11	12	13	14	15	16
	AM005-1	AM007	AM008	AM009	AM044	AM-139	AM-141-1	AM-142	AM-143	AM012	AM045	AM010	AM011	AM019	AM020	AM021
$Na_2O + K_2O$	8.73	8.59	7.70	6.94	7.10	8.13	8.20	8.02	7.80	8.10	7.41	8.12	8.19	8.58	7.12	7.06
K_2O/Na_2O	3.06	2.72	6.13	4.34	2.30	2.41	2.01	2.10	2.19	1.00	2.09	2.09	1.87	1.65	0.17	0.23
FeO*	3.28	2.64	2.20	3.47	3.96	2.27	2.71	2.38	1.55	2.55	3.78	1.41	3.68	3.00	2.75	2.83
ASI	1.20	1.18	1.17	1.50	1.18	1.10	1.10	1.03	1.20	0.96	1.09	0.98	1.02	0.93	1.10	1.03
Fe-index	0.79	0.87	0.87	0.75	0.82	0.79	0.77	0.78	0.87	0.86	0.90	0.90	0.87	0.86	0.63	0.92
MALI	8.38	8.29	7.25	6.59	5.22	7.14	7.41	7.02	7.05	6.87	5.95	7.22	7.95	7.47	6.78	6.37
Rb/Sr	7.64	8.37	11.44	8.81	2.38	4.48	4.19	3.55	31.74	7.26	6.38	21.79	17.83	3.97	0.77	0.56
Ba/Sr	20.41	7.17	6.66	17.85	9.50	8.20	10.12	7.72	2.49	10.08	7.86	4.88	6.04	4.88	1.09	2.05
$(La/Yb)_n$	6.65	5.58	4.33	6.54	7.18	9.54	7.55	6.54	2.21	5.48	5.09	1.67	2.84	4.43	6.17	9.77
Eu/Eu*	0.37	0.23	0.21	0.37	0.40	0.24	0.35	0.29	0.03	0.28	0.29	0.10	0.15	0.23	0.28	0.30
Y/Nb	3.37	4.47	6.56	5.40	4.66	3.05	4.57	3.91	2.93	6.09	5.01	5.74	7.98	4.78	4.72	3.16
T, °C	795	817	776	815	842	917	831	796	765	776	805	739	754	781	811	827

FeO* = $0.9Fe_2O_3$ + 1.1 FeO; ASI = Al/(Ca –1.67P + Na + K), Fe-index = $(FeO + 0.9\ Fe_2O_3)/(FeO + 0.9Fe_2O_3 + MgO)$, MALI = $Na_2O + K_2O{-}CaO$ (Frost B.R., Frost C.D., 2001), $(La/Yb)_n$ is chondrite-normalized ratio, Eu/Eu* = $Eu_N/[Sm_N \times Gd_N]^{1/2}$, *T*, °C, calculated crystallization temperatures of zircon (Watson and Harrison, 1983).

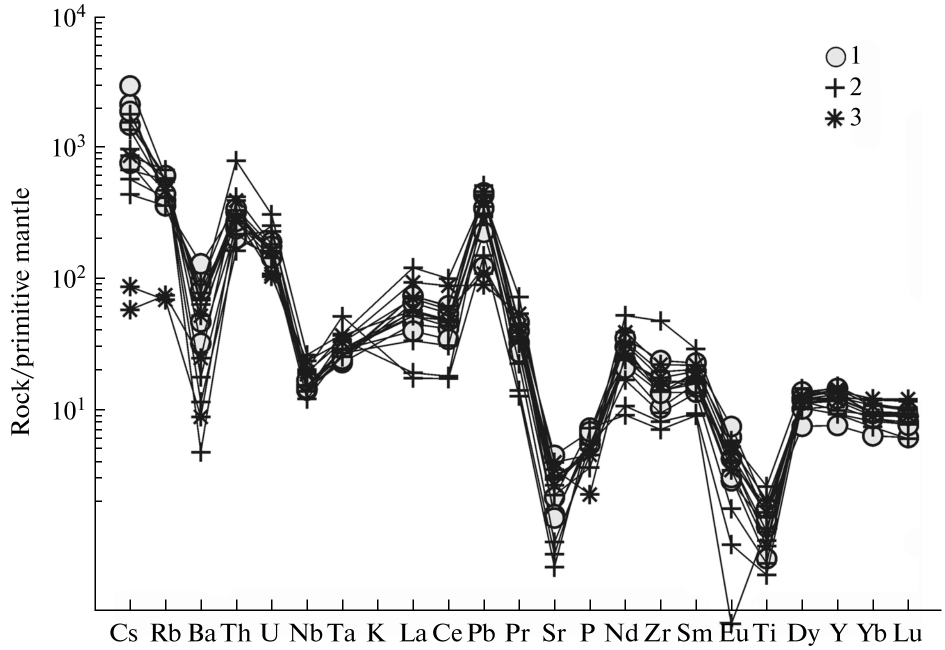

Fig. 13. Multielement diagram for the Neoproterozoic magmatic rocks of the Aktau–Mointy sialic massif. Symbols are shown in Fig. 10. The contents of minor and REE are normalized to those in primitive mantle (Sun and McDonough, 1989).

Results of Sm–Nd isotope geochemical studies of the volcanic rocks of the Altyn Syngan Formation and granites of the Uzunzhal Complex are shown in Table 4. They are characterized by $T_{Nd}(DM)$ = 1.9–1.7 Ga and negative values of $\varepsilon_{Nd}(T)$ (from –1.9 to –3.5).

DISCUSSION

Almost identical age and geochemical similarity of felsic volcanic rocks of the Aktau–Mointy Massif and granites of the Uzunzhal Complex confirm the previous assumption that these rocks are comagmatic (Avdeev et al., 1990; Degtyarev et al., 2008). This makes it possible to consider the volcanic rocks and granites as a single volcanoplutonic association, which was formed during the Neoproterozoic Tonian period (~920 Ma), after accumulation of quartzite–schist sequences. It was established that the felsic volcanic rocks of the Altyn Syngan Formation in the eastern part of the Aktau–Mointy Massif are the youngest rocks among the Proterozoic metamorphic complexes and occupy the upper structural position. The porphyroids of the Urkendeu Formation in the western part of the massif are coeval to the felsic volcanic rocks of the Altyn Syngan Formation, but experienced significant structural-metamorphic reworking with formation of large recumbent folds showing inverse stratigraphy in the overturned limbs. The disturbance of fold structure by a series of imbricated thrusts resulted in the repetition of felsic volcanic rocks and quartzite–schist sequences on the fold limbs.

Geodynamic Typification of the Volcanic Rocks and Granites

As already noted, the volcanogenic sequences of the Altyn Syngan Formation of the Aktau–Mointy Massif occupy the highest structural position in the section of its basement and with unconformity rest on the quartzite–schist sequences. In other words, the emplacement of the considered volcanoplutonic association completed the formation of the shelf quartzite–schist complexes of the Aktau–Mointy Massif and presumably was related to the within-plate magmatic activity.

The petrochemical features of the Late Riphean volcanic rocks and granites of the Aktau–Mointy Massif (ASI_{av} 1.09; $FeO/(FeO + MgO)_{av}$ 0.82; $MALI_{av}$ 7.2) resemble those of typical within-plate granites of the ferroan series according to (Frost C.D. and Frost B.R., 2011) and A-type according to (Collins et al., 1982; Clemens et al., 1986). The calculated Zr saturation temperatures (780–920°C, Watson and Harrison, 1983) indicate the high-temperature regime of their formation, which is characteristic feature of the anorogenic ferroan granites. Based on the high Y/Nb (3.3–6.5), the Late Riphean volcanic rocks and granites are ascribed to the anorogenic A-2 type granites of crustal origin (Eby, 1982).

Table 4. Results of Sm–Nd isotope study of the Neoproterozoic volcanic rocks and granites of the Uzunzhal Complex, the Aktau–Mointy Massif

Ordinal no.	Sample no.	Content, ppm		$^{147}Sm/^{144}Nd$	$^{143}Nd/^{144}Nd$ (±2SD)	$\varepsilon_{Nd}(0)$	T, Ma	$\varepsilon_{Nd}(T)$	$T_{Nd}(DM)$, Ma	Rock name
		Sm	Nd							
1	AM005-1	7.33	35.0	0.1265	0.512052 ± 7	–11.4	925	–3.1	1916	Subalkaline rhyolite of the Altyn Syngan Formation
2	AM007	7.32	34.8	0.1273	0.512098 ± 9	–10.5	925	–2.3	1853	Subalkaline rhyolite of the Altyn Syngan Formation
3	AM008	6.51	25.9	0.1521	0.512250 ± 7	–7.6	925	–2.3	1783*	Rhyolite of the Altyn Syngan Formation
4	AM009	8.12	37.9	0.1294	0.512080 ± 6	–10.9	925	–2.9	1930	Rhyolite of the Altyn Syngan Formation
5	AM044	9.48	46.2	0.1240	0.512048 ± 8	–11.5	921	–2.9	1868	Rhyodacite of the Urkendeu Formation
6	AM010	6.01	22.7	0.1603	0.512315 ± 8	–6.3	945	–1.9	1768*	Granite of the Uzunzhal Massif
7	AM011	5.75	22.2	0.1568	0.512248 ± 6	–7.6	945	–2.8	1841*	Leucogranite of the Uzunzhal Massif
8	AM012	7.07	32.2	0.1328	0.512129 ± 8	–9.9	945	–2.2	1920	Leucogranite of the Uzunzhal Massif
9	AM045	6.89	31.1	0.1339	0.512130 ± 7	–9.9	945	–2.3	1944	Leucogranite of the Uzunzhal Massif
10	AM020	8.72	43.6	0.1210	0.512005 ± 10	–12.3	917	–3.5	1879	Granite of the Shumek Massif
11	AM021	10.6	59.9	0.1072	0.511941 ± 7	–13.6	917	–3.1	1727	Granite of the Shumek Massif

ε_{Nd} values were calculated using following parameters of the chondrite uniform reservoir (CHUR): $^{147}Sm/^{144}Nd = 0.1967$; $^{143}Nd/^{144}Nd = 0.512638$ (Jacobsen and Wasserburg, 1984). Model age $T_{Nd}(DM)$ was calculated using following parameters of the present-day depleted mantle: $^{147}Sm/^{144}Nd = 0.2137$, $^{143}Nd/^{144}Nd = 0.513151$ (Goldstein and Jacobsen, 1988); Values $T_{Nd}(DM)$, noted by * were calculated using two-stage model (Liew and Hofmann, 1988) at average $^{147}Sm/^{144}Nd$ of 0.12 in continental crust (Taylor and McLennan, 1988).

Sources of Parental Melts and Mechanisms of Their Formation

The affiliation of the Neoproterozoic anorogenic felsic volcanic rocks and granites of the Aktau–Mointy Massif to a single volcanoplutonic association suggests that they were derived through evolution of compositionally similar parental melts. As seen from Fig. 14 and Table 2, an increase of SiO_2 in the volcanic rocks and granites of this association is accompanied by the decrease of TiO_2, Al_2O_3, FeO*, FeO* + MgO, increase of K_2O, and decrease of Rb/Sr ratio, which is possibly caused by the differentiation of primary melts. This implies that volcanic rocks most close in composition to the primary melt should have the highest content of practically all major components (except for SiO_2 and K_2O), as well as Ba, Sr, and correspondingly, elevated Rb/Sr ratios. The rhyodacites of the Urkendeu Formation most completely meet this requirement (Table 2, sample AM-044). In addition, they are characterized by the highest REE content and least differentiated REE distribution (ΣREE 267, $(La/Yb)_n$ 7.2), as well as slight Eu anomaly (Eu/Eu* 0.4). On this basis, the rhyodacites may be regarded as the least differentiated volcanic rocks of the Altyn Syngan Formation, and hence, in first approximation, as parental melt for the Neoproterozoic volcanoplutonic association of the Aktau–Mointy Massif.

Experimental data show that melts compositionally similar to the rhyodacites of the Altyn Syngan Formation may arise by melting of biotite plagiogneisses (metagraywackes) (*Qtz*(40%) + *Pl*(An_{32})(32%) + *Bt*(25%) + *Ap* + *Zrn* + *Mnz* + *Tur*) or amphibole–biotite orthogneisses (*Pl*(48.2%) + *Qtz*(30%) + *Bt*(19.4%) + *Amph*(1.8%) + *Ep* + *Ap* + *Zrn*) of tonalitic composition at temperature > 940°C and P = 8–10 kbar (Skjerlie et al., 1993; Vielzeuf and Montel, 1994; Montel and Vielzeuf, 1997). An impact of a powerful heat source on the lower continental crust is required to produce the within-plate Neoproterozoic magmatic rocks of the Aktau–Mointy Massif. This source of heat could be underlplating mafic melts (hot spot or mantle plume derivatives), which caused the granulite-facies metamorphism and partial melting of the lower continental crust (Ellis, 1987; Rudnick and Fountain, 1995).

Results of Sm–Nd isotope-geochemical studies of the volcanic rocks of the Altyn Syngan Formation and granites of the Uzunzhal Complex (T_{Nd}(DM) = 1.9–1.7 Ga, ε_{Nd}(T) from –1.9 to –3.5) indicate that their parental melts were derived by melting of the Paleoproterozoic crust, possibly with a minor addition of the younger mantle-derived material. The wide distribution of thick shelf quartz-schist sequences within the Precambrian sialic massifs of Kazakhstan and Northern Tianshan indicates that these massifs, including the Aktau–Mointy one, were accumulated on a thick mature continental crust. This conclusion is confirmed by Sm–Nd isotope-geochemical data, which testify that the sialic massifs of Kazakhstan and Northern Tianshan bear significant contribution of the Paleoproterozoic continental crust. In particular, the Mesoproterozoic granitoids (1153–1133 Ma) of the Makbal block, Northern Tianshan, are characterized by the Paleoproterozoic Nd model ages (T_{Nd}(DM) 2.1–1.7 Ga, Kröner et al., 2013). The Mesoproterozoic granitoids (1150 Ma) of the Kokchetav Massif have T_{Nd}(DM) 2.5–2.3 Ga (Tretyakov et al., 2011a, Turkina et al., 2011). The Neoproterozoic (844–834 Ma) granitoids and orthogneisses of the Aktyuz Block, Northern Tianshan, also have Paleoproterozoic Nd model ages (T_{Nd}(DM) 2.2–1.6 Ga; Kröner et al., 2012).

Among the oldest known sialic massifs in the Precambrian complexes of Kazakhstan and Northern Tianshan are the Mesoproterozoic granites of the Makbal and Kochkor blocks of Northern Tianshan (Degtyarev et al., 2011; Kröner et al., 2013) and almost coeval granites and felsic volcanic rocks of the Kokchetav Massif (Tretyakov et al., 2011a, 2011b; Turkina, 2011). The older metamorphic and magmatic complexes at the present-day erosion surface of the Precambrian sialic massifs of Kazakhstan and Northern Tianshan have not been reliably established yet. Arbitrarily, these are the metamorphic rocks of the Aidaly (Chuya–Kendyk Tas Massif), Anrakhai (Dzhel'tau Massif), Bekturgan (Ulutau Massif), and Zerenda (Kokchetav Massif) groups (*Rannii dokembrii...*, 1993), which are regarded as the fragments of the Early Precambrian continental crust exhumed during Early Paleozoic subduction–collisional events (Maruyama and Parcinson, 2000; Dobretsov et al., 2005; Alexeiev et al., 2011). The aforementioned complexes are made up mainly of two-mica, biotite, garnet–biotite paragneisses and felsic orthogneisses, and, taking into account experimental data (Montel and Vielzeuf, 1997; Skjerlie et al., 1993), may be considered as possible source for crustal granitoid melts, which were parental for magmatic rocks of the Neoproterozoic volcanoplutonic association of the Aktau–Mointy Massif.

Paleotectonic Position of the Aktau–Mointy Massif in the Late Riphean

The terminal stage in the Precambrian tectonomagmatic evolution of the Aktau–Mointy Massif was marked by the accumulation of shelf quartzite–schist sequences and formation of the Neoproterozoic anorogenic volcanoplutonic rhyolite–granite association. Taking into account the unconformable deposition of the volcanic rocks of the Altyn Syngan Formation on the rocks of the quartzite–schist sequences, the obtained age value of 925 ± 9 Ma in first approximation corresponds to the upper age boundary of their formation. Analogues of the quartzite–schist sequences of the Aktau–Mointy Massif are also widely spread in other sialic massifs of Northern Kazakhstan

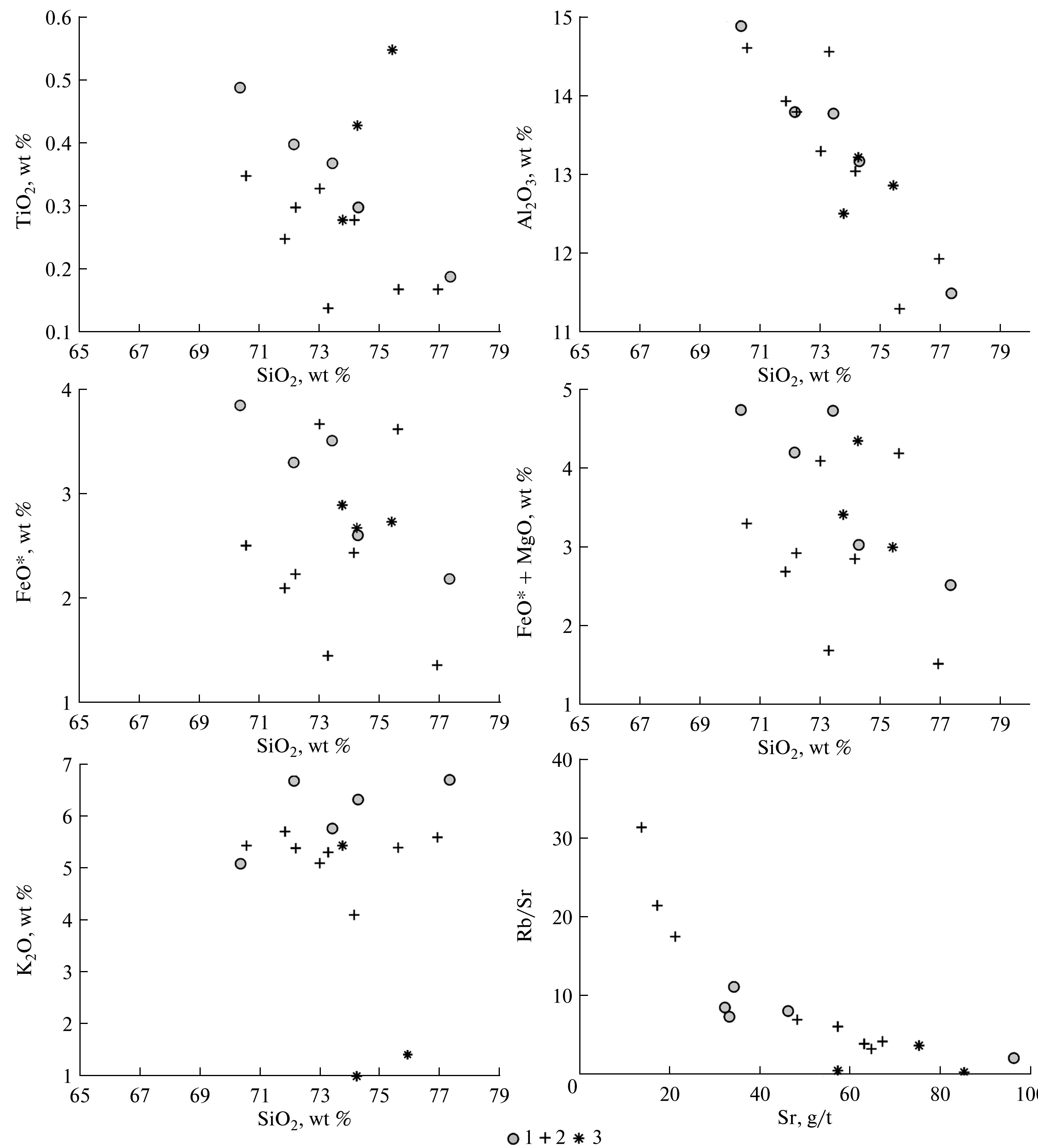

Fig. 14. Variation diagrams for the Neoproterozoic magmatic rocks of the Aktau–Mointy sialic massif. Symbols are shown in Fig. 10.

(Kokchetav, Ishkeol'mes, and Erementau-Niyaz ones), where they are underlain by different metamorphic and magmatic rocks. In the Kokchetav massif, the quartzite–schist sequence rests on the 1136 ± 4 Ma trachyrhyolites (Tretyakov et al., 2011a). This age estimation constrains the lower age boundary of the quartzite–schist sequences of the massif, which have accumulated within the interval from the terminal Mesoproterozoic to the beginning of the Neoproterozoic. This is confirmed by age data on the detrital zircons from quartzites of the Kokchetav and Erementau–Niyaz massifs (Letnikov et al., 2001; Kovach et al., 2014).

The fact that many sialic massifs in the western CAFB contains the Meso-Neoproterozoic subplatform quartzite–schist complexes suggests that they belonged to a single large continental block that formed at the end of the Mesoproterozoic (Degtyarev et al., 1998). However, the Late Precambrian magmatic activity was not simultaneous in different massifs. The 1150–1000 Ma-old Stenian (Kokchetav and Ishkeol'mes massifs, western part of the Northern Tianshan) and 800–750 Ma-old Cryogenian (Ulutau, Chuya Kendyk Tas, Karatau-Talass, and the eastern part of the Northern Tianshan massifs) complexes are the widest spread among the magmatic complexes of this age in the western CAFB. The manifestation of the Tonian (925–920 Ma) magmatism is a distinctive feature of the Aktau–Mointy Massif, which has no age analogues in the western CAFB.

After termination of the Tonian magmatism in the Ediacaran and Early Paleozoic, the Aktau–Mointy Massif was overlain by terrigenous–carbonate cover, with terrigenous rocks and tilloids at the base. The cover complexes of similar composition, structure, and age have been also formed at that time within other sialic massifs of Kazakhstan and Tianshan, as well as Central Mongolia. The best studied cover complexes are those of the Dzabkhan Massif in Central Mongolia, where the Upper Precambrian–Lower Paleozoic terrigenous–carbonate cover with unconformity lies on the felsic volcanic rocks of the Cryogenian Dzabkhan Formation (around 800 Ma) intruded by alkali granites with an age around 755 Ma (Levashova et al., 2011; Yarmolyuk et al., 2008). The base of the cover succession consists of tillites of the Taishir Formation, which are overlain by the limestones of the Tsaganalom Formation with basal zone dated at 632 ± 14 Ma (Ovchinnikova et al., 2012), and Cambrian terrigenous–carbonate rocks. In the Aktau–Mointy Massif, their counterparts are the tilloids of the Kapal Formation and the carbonate rocks of the Basagin Group of the Ediacaran–Lower Cambrian age (Al'perovich, 1971; Filatova, 1990; Filatova et al., 1992).

At present, the determination of paleotectonic position of definite continental block is mainly based on the formation affiliation of its complexes, their age, and results of paleomagnetic studies. Unfortunately, the paleomagnetic data on the Precambrian complexes of CAFB are fragmentary (Levashova et al., 2011). Therefore, paleotectonic setting may be reconstructed only from composition, structure, and age of the Precambrian stratified and plutonic rocks.

According to the existing paleotectonic reconstructions, continental block that included the sialic massifs of western CAFB was a part of Rodinia in the Late Precambrian. The assembly of this supercontinent was caused by the Grenville orogeny, the main phases of which occurred in the Mesoproterozoic within 1300–1000 Ma (Li et al., 2008; Bogdanova et al., 2009). The beginning of the Rodinia break-up is regarded to be caused by the activation of the within-plate magmatism in the middle Neoproterozoic (around 830 Ma) (Li et al., 2008; Bogdanova et al., 2009). The earlier Neoproterozic events, including the within–plate magmatism of the Aktau–Mointy Massif, occurred mainly in the southern part of the Rodinia supercontinent (Fig. 15). In this region, the Late Precambrian within-plate processes were expressed in the continental rifting on the passive margin of the São Francisco craton (Brito Neves et al., 1999; Correa-Gomes and Oliviera, 2000; Stern, 2008). The riftogenic complexes are of Stenian age and include terrigenous and volcanogenic rocks of the Espinhaço Supergroup (Alkmim and Martins-Neto, 2012). Their formation was accompanied by the emplacement of layered mafic-ultramafic intrusions and tholeiitic dolerite dike swarm with an age of 1100–1000 Ma (Correa-Gomes and Oliveira, 2000; Angeli et al., 2004; Tupinambá et al., 2007). The Neoproterozoic complexes of the Aktau–Mointy Massif in age and composition are most close to the Tonian riftogenic complexes in the western Congo Craton (West Congo belt). During this time, quartzite–sandy and black shale sequences were accumulated there (Zadinian Group), after the formation of the trachyrhyolites and alkali granites with an age of 1000 Ma (Tack et al., 2001). The younger rocks are represented by felsic volcanogenic-sedimentary sequence (Mayumbian Group), high-K trachyrhyolites (Inga metarhyolites with an age of 920–912 Ma), and comagmatic (924–917 Ma) anorogenic granosyenites, monzogranites, and granites (Tack et al., 2001).

These events were followed by the subsidence of the western flank of the Congo Craton and the formation of terrigenous–carbonate sequences (lower part of the West Congo Group) (Tack et al., 2001; Kadima et al., 2011). These events are correlated with the opening of the Macaúbas paleobasin between the Congo and São Francisco cratons (Eriksson et al., 2001; Sial et al., 2010; Pedrosa-Soares and Alkmim, 2011; Alkmim and Martins-Neto, 2012). In the São Francisco craton, its opening was preceded by the activation of within-plate magmatism and intrusion of tholeiitic dike swarms with an age approximately 920 Ma (Eriksson et al., 2001; Tupinambá et al., 2007). The incipient opening of the basin was marked by the rift magmatism responsible for the formation of anorogenic granitoid intrusions and basic rocks in the Araçuaí belt (Pedrosa-Soares and Alkmim, 2011; Silva et al., 2008). The timing of maximum opening of the basin is defined by the age of ophiolites (800 Ma) (Pedrosa-Soares and Alkmim, 2011; Alkmim and Martins-Neto, 2012). The paleobasin continued to evolve during the entire Cryogenian, with transition from pre-rift and rift stage to the passive margin. The complexes of the latter are represented by the

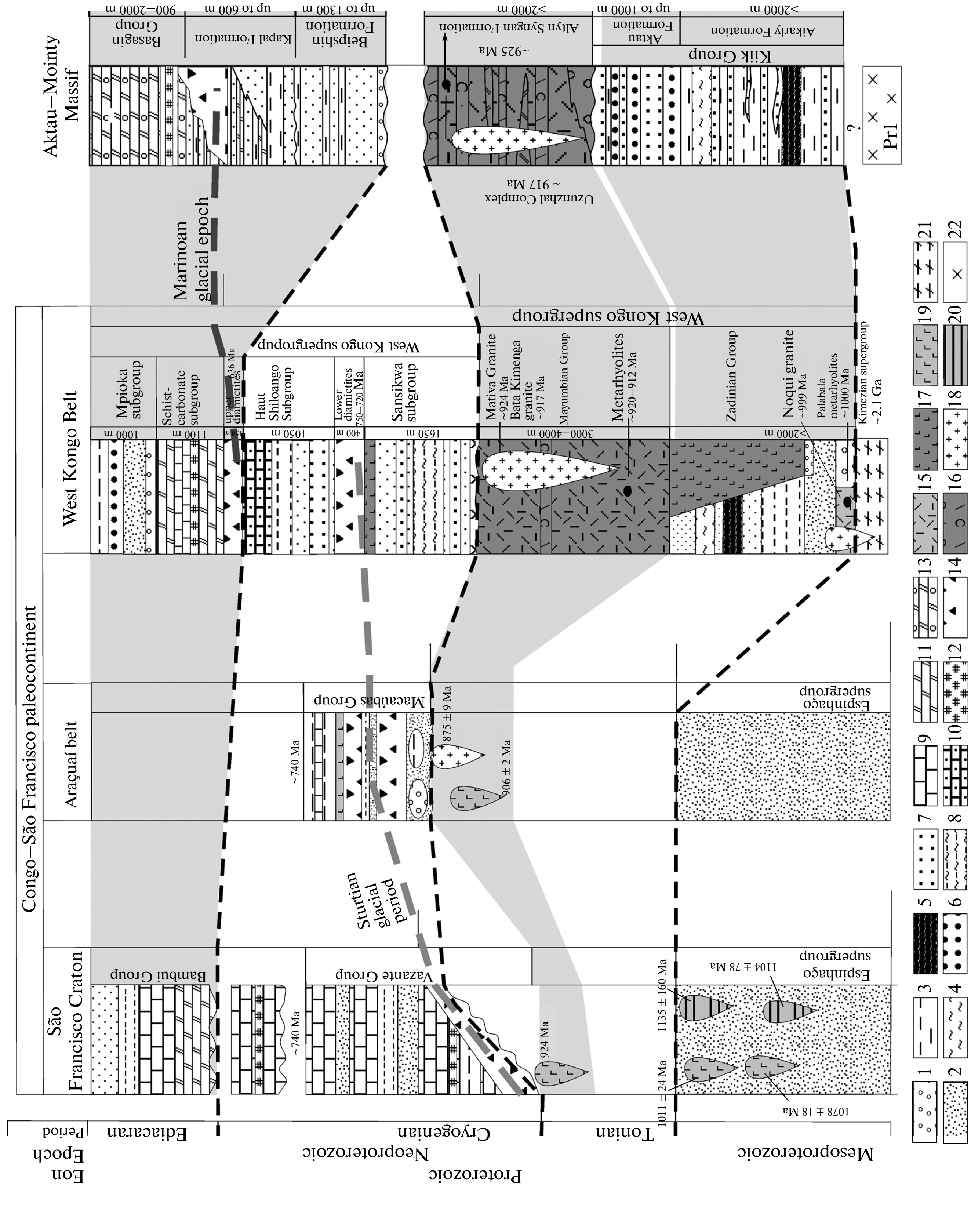
Eon
Epoch
Period
Proterozoic
Neoproterozoic
Mesoproterozoic
Ediacaran
Cryogenian
Tonian
Congo–São Francisco paleocontinent
São Francisco Craton
Araçuaí belt
West Kongo Belt
Aktau–Mointy Massif
Sturtian glacial period
Marinoan glacial epoch
Bambuí Group
Vazante Group
Espinhaço supergroup
Macaúbas Group
West Kongo supergroup
Mpioka subgroup
Schist-carbonate subgroup
Haut Shiloango Subgroup
Sansikwa subgroup
Zadinian Group
Mayumbian Group
Kiik Group
Aikarly Formation
Aktau Formation
Altyn Syngan Formation
Beipshin Formation
Kapal Formation
Basagin Group
Uzunzhal Complex ~ 917 Ma

Fig. 15. Generalized correlation scheme of the Late Precambrian stratified and magmatic complexes of the São Francisco Craton, Araçuaí and West Congo belts, and Aktau–Mointy sialic massif. Compiled using materials of (Zaitsev et al., 1980; Besstrashnov et al., 1989; Filatova et al., 1992; Apollonov et al., 1999; Córrea-Gormes and Oliviera, 2000; Eriksson et al., 2001; Tack et al., 2001; Angeli et al., 2004; Degtyarev et al., 2003; Tupinambá et al., 2007; Degtyarev et al., 2008; Sial et al., 2010; Kadima et al., 2011; Pedrosa-Soares and Alkmim, 2011; Alkmim and Martins-Neto, 2012; Brito Neves et al., 1999; Silva et al., 2008). (1) Conglomerates, (2) sandstones; (3) siltstones, (4) schists; (5) black shales, (6) quartzites, (7) quartzitic sandstones, (8) quartzite schists, (9) limestones, (10) calcarenites, (11) dolomites, (12) phosphorites, (13) onkolitic dolomites; (14) tillites, (15) rhyolites, trachyrhyolites, (16) felsic tuffs, (17) basalts, (18) granitoids, (19) basic dikes, (20) layered intrusions, (21) crystalline basement complexes, (22) Paleoproterozoic complexes of the Aktau–Mointy sialic massif as inferred from Sm–Nd isotope data.

Macaúbas Group in the Araúaí belt and the lower part of the West Congo Group. In the São Francisco Craton, their facies analogues are basal diamictitic sequences (Jequitaí Formation) and overlying terrigenous–carbonate sequences (Vazante Group) (Alkmim and Marthins-Neto, 2012). Within the Aktau–Mointy Massif, this age interval corresponds to the accumulation of the Beipshin Formation, the terrigenous sequences of which with conglomerates at the base rest on the Tonian volcanic rocks of the Altyn Syngan Formation (Filatova, 1990).

The Ediacaran stage in the evolution of the São Francisco and West Congo cratons is related to the Brazilian–Pan-African orogeny, beginning of the closure of the Macaúbas paleobasin (630 Ma), and formation of the Araçuaí–West Congo orogen (580 Ma) (Eriksson et al., 2001). The stratified complexes of this age are represented by dolomitic and clayey–carbonate sequences with tillite horizons at the lower portions (correspondingly, the Bambui Group and the upper part of the West Congo Group) (Tack et al., 2001; Sial et al., 2010; Kadima et al., 2011; Alkmim and Martins-Neto, 2012). Within the Aktau–Mointy and Dzabkhan massifs, the analogues of these complexes are the Kopal and Basagin formations and the Tsaganalom Formation, respectively.

Recently obtained data indicate the formation of the Xu-Huai riftogenic system, which is traced by subalkaline basic dikes of the Tonian (920–900 Ma) age in the northeastern part of the North China Craton (Peng Peng et al., 2011a, 2011b). This suggests a genetic link between manifestations of the Tonian plume magmatism in the São Francisco and West Congo cratons, North China Craton, and the Araçuaí belt, which are ascribed to the incipient break-up of the Rodinian supercontinent (Peng Peng et al., 2011a, 2011b).

Presented data demonstrate the great similarity between the geological evolution of the Aktau–Mointy Massif and cratons in the southern part of the Rodinian supercontinent, in particular, in the Congo–São-Francisco paleocontinent. Thus, the Late Precambrian evolution of the Aktau–Mointy Massif heralds the global-scale divergent processes within the indicated paleocontinent.

CONCLUSIONS

(1) The felsic volcanic rocks of the Altyn Syngan and Urkendeu formations and granites of the Uzunzhal Complex of the Aktau–Mointy sialic massif are ascribed to a single anorogenic rhyolite–granite volcanoplutonic association, which was formed during the Neoproterozoic Tonian period (~ 920 Ma) and completed the formation of the Precamrbian continental crust of this massif.

(2) The anorogenic rhyolite–granite volcanoplutonic association of the Aktau–Mointy sialic massif was presumably derived by melting of the Paleoproterozoc continental crust represented by metagraywackes and orthogneisses of the tonalitic composition at temperature more than 940°C and $P = 8$–10 kbar under the impact of mantle hot spot or plume.

(3) The formation of the Tonian anorogenic volcanoplutonic association of the Aktau–Mointy sialic massif heralds the global-scale divergent processes within the southern part of the Rodinian supercontinent (Congo–São Francisco paleocontinent).

ACKNOWLEDGMENTS

This work was supported by the Russian Foundation for Basic Research (project nos. 14-05-00920 and 12-05-33069-mol-a-ved), a Grant of the President of the Russian Federation (no. Mk-766.2013.5), and the Earth Science Division of the Russian Academy of Sciences (Program "Geodynamic Evolution of Lithotectonic Complexes of the Folded Belts in the Neogean")

REFERENCES

Al'perovich, E.V., Ancient carbonate sequences of the northwestern Balkhash region, in *Stratigrafiya dokembriya Kazakhstana i Tyan'-Shanya* (Precambrian Stratigraphy of Kazakhstan and Tianshan), Moscow: MGU, 1971, pp. 90–96.

Alexeiev, D.V., Ryazantsev, A.V., Kröner, A., et al., Geochemical data and zircon ages for rocks in a high-pressure belt of Chu-Yili mountains, southern Kazakhstan: implications for the earliest stages of accretion in Kazakhstan and the Tianshan, *J. Asian Earth Sci.*, 2011, vol. 42, pp. 805–820.

Alkmim, F.F. and Martins-Neto, M.A., Proterozoic first-order sedimentary sequences of the São Francisco Craton, eastern Brazil, *Mar. Petrol. Geol.*, 2012, vol. 33, pp. 127–139.

Angeli, N., Teixeira, W., Heaman, L., et al., Geochronology of the Ipanema layered mafic-ultramafic complex, Minas Gerais, Brazil: evidence of extension at the Meso-Neoproterozoic time boundary, *Int. Geol. Rev.*, 2004, vol. 46, pp. 730–744.

Apollonov, M.K., Zhemchuzhnikov, V.G., and Dubinina, S.V., Ordovician of the northwestern Balkhash region, *Izv. Akad. Nauk Kaz. SSR, Ser. Geol.,* 1990, no. 4, pp. 3–16.

Avdeev, A.V., On age of the porphyroids of the Atasu-Mointy watershed, in *Stratigrafiya nizhnepaleozoiskikh i siluriiskikh otlozhenii Tsentral'nogo Kazakhstana* (Stratigraphy of the Lower Paleozoic and Silurian Deposits of the Central Kazakhstan), Leningrad: Nedra, 1965, pp. 22–25.

Avdeev, A.V., Al'perovich, E.V., Voznesenskii, V.D., and Koren'kov, B.G., Precambrian deposits of the Aktau-Mointy watershed, in *Dopaleozoi i paleozoi Kazakhstana* (Pre-Paleozoic and Paleozoic of Kazakhstan), Alma-Ata: Nauka, 1974, vol. 1, pp. 53–57.

Avdeev, A.V. and Kovalev, A.A., *Ofiolity i evolyutsiya yugozapadnoi chasti Uralo-Mongol'skogo skladchatogo poyasa* (Ophiolites and Evolution of the Southwestern Ural–Mongolian Fold Belt), Moscow: Izd-vo MGU, 1989.

Avdeev, A.V., Zlobin, G.N., Kim, V.S., et al., New age data on the Precambrian rhyolite–granite associations of the Atasu-Mointy watershed (Central Kazakhstan), *Dokl. Akad. Nauk SSSR,* 1990, vol. 311, no. 3, pp. 685–689.

Besstrashnov, V.M., Gerasimova, N.A., and Kurkovskaya, L.A., Ordovician stratigraphy of the Aktau-Mointy uplift, in *Stratigrafiya paleozoya Kazakhstana* (Paleozoic Stratigraphy of Kazakhstan), Alma-Ata: Nauka, 1989, pp. 68–77.

Bogdanova, S.V., Pisarevsky, S.A., and Li, Z.X., Assembly and breakup of Rodinia (some results of IGCP Project 440), *Stratigr. Geol. Correlation*, 2009, vol. 17, no. 3, pp. 259–274.

Brito Neves B.B., Campos Neto M., and Fuck, R.A., From Rodinia to western Gondwana: an approach to the Brasiliano–Pan African cycle and orogenic collage, *Episodes*, 1999, vol. 22, pp. 155–166.

Clemens, J.D., Holloway, J.R., and White, A.J.R., Origin of an A-type granite: experimental constraints, *Am. Mineral.*, 1986, vol. 71, pp. 317–324.

Collins, W.J., Beams, D., White, J.R., and Chappell, B.W., Nature and origin of A-type granites with particular reference to south-eastern Australia, *Contrib. Mineral. Petrol.*, 1982, vol. 80, pp. 189–200.

Côrrea-Gomes, L.C. and Oliveira, E.P., Radiating 1.0 Ga mafic dyke swarms of eastern Brazil and western Africa: evidence of post-assembly extension in the Rodinia Supercontinent?, *Gondwana Res.*, 2000, vol. 3, pp. 325–332.

Degtyarev, K.E., Position of the Aqtau–Dzungar microcontinent in the structural framework of the Paleozoides of central Kazakhstan, *Geotectonics*, 2003, vol. 37, no. 4, pp. 271–288.

Degtyarev, K.E., Shatagin, K.N., Kuznetsov, N.B., and Astrakhantsev, O.V., Platform stage in the Precambrian evolution of Kazakhstan: paleotectonic, paleogeographical, and geochronological aspects, in *Paleogeografiya venda - rannego paleozoya Severnoi Evrazii* (Vendian–Early Paleozoic Paleogeography of North Eurasia), Yekaterinburg: UrO RAN, 1998, pp. 159–166.

Degtyarev, K.E. and Ryazantsev, A.V., Cambrian arc–continent collision in the Paleozoides of Kazakhstan, *Geotectonics,* 2007, vol. 41, no. 1, pp. 63–85.

Degtyarev, K.E., Shatagin, K.N., Kotov, A.B., et al., Late Precambrian volcanoplutonic association of the Aktau–Dzhungar Massif, central Kazakhstan: structural position and age, *Dokl. Earth Sci.*, 2008, vol. 421A, pp. 879–883.

Degtyarev, K.E., Tret'yakov, A.A., Ryazantsev, A.V., et al., Stenian granitoids of the West Kyrgyz Ridge (North Tianshan): position, structure, and age determination, *Dokl. Earth Sci.*, 2011, vol. 441, no. 2, pp. 1484–1488.

Degtyarev, K.E., *Tektonicheskaya evolyutsiya rannepaleozoiskikh ostrovoduzhnykh sistem i formirovanie kontinental'noi kory kaledonid Kazakhstana* (Tectonic Evolution of the Early Paleozoic island arc systems and formation of continental crust of Kazakhstan Caledonides), Moscow: GEOS, 2012.

Dobretsov, N.L., Buslov, M.M., Zhimulev, F.I., et al., Vendian–Early Ordovician geodynamic evolution and model for exhumation of ultra-high and high-pressure rocks from the Kokchetav subduction–collision zone (northern Kazakhstan), *Russ. Geol. Geophys.,* 2006, vol. 47, no. 4, pp. 424–440.

Eby, G.N., Chemical subdivision of the A-type granitoids: petrogenetic and tectonic implications, *Geology*, 1992, vol. 20, pp. 641–644.

Ellis, D.J., Origin and evolution of granulites in normal and thickened crusts, *Geology*, 1987, vol. 15, pp. 167–170.

Eriksson, P.G., Martins-Neto, M.A., Nelson, D.R., et al., An introduction to Precambrian basins: their characteristics and genesis, *Sediment. Geol.*, 2001, vol. 141–142, pp. 1–35.

Filatova, L.I., Gvozdik, N.I., and Zubatkina, G.M., Proterozoic stratigraphy of Central Kazakhstan, in *Geologiya i poleznye iskopaemye Tsentral'nogo Kazakhstana* (Geology and Mineral Resources of Central Kazakhstan), Moscow: Nauka, 1988.

Filatova, L.I., Upper Cambrian stratigraphy of southeast Central Kazakhstan, *Vestn. Mosk. Univ., Ser. Geol.*, 1990, no. 1, pp. 3–16.

Filatova, L.I., Zubatkina, G.M., and Stepanov, Yu.B., Upper Proterozoic–Lower Cambrian successions of southeastern Central Kazakhstan, in *Stratigrafiya, litologiya, geokhimiya i rudonosnost' verkhnego rifeya-venda Srednei Azii, Kazakhstana, Sibiri* (Stratigraphy, Lithology, Geochemistry, and Ore Potential of the Riphean–Vendian of Middle Asia, Kazakhstan, and Siberia), Bishkek: Ilim, 1992, pp. 37–66.

Frost, B.R. and Frost, C.D., A geochemical classification for feldspathic igneous rocks, *J. Petrol.*, 2001, vol. 49, pp. 1955–1969.

Frost, C.D. and Frost, B.R., On ferroan (A-type) granitoids: their compositional variability and modes of origin, *J. Petrol.*, 2011, vol. 52, no. 1, pp. 39–53.

Geologicheskaya karta Kazakhskoi SSR. Masshtab 1 : 500000. Seriya Tsentral'no-Kazakhstanskaya. Ob''yasnitel'naya zapiska (Geological Map of the Kazakh ASSR. Scale 1 : 500000. Central Kazakhstan Series. Explanatory Note), Alma-Ata, 1981.

German, L.L. and Filippovich, I.Z., Metamorphism and granitization in the Precambrian of the Atasu-Mointy watershed (Central Kazakhstan), *Izv. Akad. Nauk SSSR, Ser. Geol.*, 1987, no. 9, pp. 41–55.

Goldstein, S.J. and Jacobsen, S.B., Nd and Sr isotopic systematic of river water suspended material: implications for crustal evolution, *Earth Planet. Sci. Lett.*, 1988, vol. 87, no. 3, pp. 249–265.

Jacobsen, S.B. and Wasserburg, G.J., Sm-Nd isotopic evolution of chondrites and achondrites, *Earth Planet. Sci. Lett.*, 1984, vol. 67, no. 2, pp. 137–150.

Kadima, E., Delvaux, D., Sebagenzi, S.N., et al., Structure and geological history of the Congo Basin: an integrated interpretation of gravity, magnetic and reflection seismic data, *Basin Res.*, 2011, vol. 23, pp. 499–527.

Kovach, V.P., Ryazantsev, A.V., Tretyakov, A.A., et al., U–Pb age of detrital zircons from Neoproterozoic Placers of the Erementau–Niyaz Massif as a reflection of stages of Precambrian tectono-magmatic evolution of Northern Kazakhstan, *Dokl. Akad. Nauk*, 2014, vol. 455, no. 1, pp. 254–258.

Kröner, A., Hegner, E., Lehmann, B., et al., Paleozoic arc magmatism in the Central Asian orogenic belt of Kazakhstan: SHRIMP zircon and whole-rock Nd isotopic systematic, *J. Asian Earth Sci.*, 2008, no. 32, pp. 118–130.

Kröner, A., Alexeiev, D.V., Hegner, E., et al., Zircon and muscovite ages, geochemistry, and Nd–Hf isotopes for the Aktyuz metamorphic terrane: evidence for an Early Ordovician collisional belt in the northern Tianshan of Kyrgyzstan, *Gondwana Res.*, 2012, vol. 21, pp. 901–927.

Kröner, A., Alexeiev, D.V., Rojas-Agramonte, Y., et al., Mesoproterozoic (Grenville-age) terranes in the Kyrgyz north Tianshan: zircon ages and Nd–Hf isotopic constraints on the origin and evolution of basement blocks in the southern Central Asian Orogen, *Gondwana Res.*, 2013, vol. 23, pp. 272–295.

Krogh, T.E., A low-contamination method for hydrothermal decomposition of zircon and extraction of U and Pb for isotopic age determination, *Geochim. Cosmochim. Acta*, 1972, vol. 37, pp. 485–494.

Krogh, T.E., Improved accuracy of U-Pb zircon by the creation of more concordant systems using an air abrasion technique, *Geochim. Cosmochim. Acta*, 1982, vol. 46, pp. 637–649.

Larionova, Yu.O., Samsonov, A.V., and Shatagin, K.N., Sources of Archean sanukitoids (high-Mg subalkaline granitoids) in the Karelian Craton: Sm-Nd and Rb-Sr isotopic-geochemical evidence, *Petrology,* 2007, vol. 15, no. 6, pp. 530–550.

Letnikov, F.A., Watanabe, T., Kotov, A.B., et al., Problem of the age of metamorphic rocks of the Kokchetav Block, Northern Kazakhstan, *Dokl. Earth Sci.*, 2001, vol. 381, pp. 1025–1027.

Levashova, N.M., Gibsher, A.S., Meert, J.G., and Gric, W.C., The origin of the Central Asian orogenic belt microcontinents: constraints from paleomagnetism and geochronology, *Precambrian Res.*, 2011, vol. 185, pp. 37–54.

Levashova, N.M., Gibsher, A.S., and Meert, J.G., Precambrian microcontinents of the Ural–Mongolian Belt: new paleomagnetic and geochronological data, *Geotectonics,* 2011, vol. 45, no. 1, pp. 51–70.

Li, Z.X., Li, X.H., Kinny, P.D., and Wang, J., The breakup of Rodinia: did it start with a mantle plume beneath South China?, *Earth Planet. Sci. Lett*, 1999, vol. 173, pp. 171–181.

Li, Z.X., Bogdanova, S.V., Collins, A.S., et al., Assembly, configuration, and break-up history of Rodinia: a synthesis, *Precambrian Res.*, 2008, vol. 160, pp. 179–210.

Liew, T.C. and Hofmann, A.W., Precambrian crustal components, plutonic associations, plate environment of the Hercynian Fold Belt of central Europe: indications from a Nd and Sr isotopic study, *Contrib. Mineral. Petrol.*, 1988, vol. 98, no. 2, pp. 129–138.

Ludwig, K.R., PbDat. Version 1.21, *U.S. Geol. Surv. Open-File Rept.*, 1991, no. 88-542.

Ludwig, K.R., Isoplot/Ex. Version 2.06. A geochronological toolkit for Mircosoft Excel, *Berkley Geochronol. Center Sp. Publ.*, 1999, no. 1a.

Maruyama, S. and Parcinson, C.D., Overview of the geology, petrology and tectonic framework of the HP-UHP metamorphic belt of the Kokchetav Massif, Kazakhstan, *The Island Arc*, 2000, no. 9, pp. 439–455.

Mattinson, J.M., A study of complex discordance in zircons using step-wise dissolution techniques, *Contrib. Mineral. Petrol.*, 1994, vol. 116, pp. 117–129.

Montel, J.-M. and Vielzeuf, D., Partial melting of metagreywackes. Part II. Compositions of minerals and melts, *Contrib. Mineral. Petrol.*, 1997, vol. 128, pp. 176–196.

Ovchinnikova, G.V., Kuznetsov, A.B., Vasil'eva, I.M., et al., U–Pb Age and Sr isotope signature of cap limestones from the Neoproterozoic Tsagaan Oloom Formation, Dzabkhan River basin, Western Mongolia, *Stratigr. Geol. Correlation*, 2012, vol. 20, no. 6, pp. 516–527.

Pedrosa-Soares, A.C., Alkmim de, F.F., How many rifting events preceded the development of the Araçuaí–West Congo Orogen?, *Geonomos*, 2011, vol. 19, no. 2, pp. 244–251.

Peng, Peng., Bleeker, W., Ernst, R.E., et al., U-Pb baddeleyite ages, distribution and geochemistry of 925 Ma mafic dykes and 900 Ma sills in the North China Craton: evidence for a Neoproterozoic mantle plume, *Lithos*, 2011a, vol. 127, pp. 210–221.

Peng, Peng., Zhai, M.-G., Li, Q., et al., Neoproterozoic (~900 Ma) Sariwon sills in North Korea: geochronology, geochemistry and implications for the evolution of the south-eastern margin of the North China Craton, *Gondwana Res.*, 2011b, vol. 33, pp. 267–309.

Rannii dokembrii Tsentral'no-Aziatskogo skladchatogo poyasa (Early Precambrian of the Central Asian Fold Belt), St. Petersburg: Nauka, 1993, p. 272.

Rudnick, R.L. and Fountain, D.M., Nature and composition of the continental crust—a lower crustal perspective, *Rev. Geophys.*, 1995, vol. 33, pp. 267–309.

Sial, A.N., Dardenne, M.A., Misi, A., et al., The São Francisco Palaeocontinent, in *Neoproterozoic–Cambrian Tectonics, Global Change and Evolution: A Focus On Southwestern Gondwana, Develop. Precambrian Geol.*, Gaucher C., Sial A., Halverson G., and Frimmel, H., Eds., 2010, vol. 16, pp. 31–69.

Silva, L.C., Pedrosa-Soares, A.C., Teixeira, L., and Armstrong, R., Tonian rift-related, A-type continental plutonism in the Araçuaí Orogen, eastern Brazil: new evidence for the breakup stage of the São Francisco–Congo paleocontinent, *Gondwana Res.*, 2008, vol. 13, pp. 527–53.

Skjerlie, K.P., Skjerlie, K.P., and Johnston, A.D., Fluid-absent melting behavior of an F-rich tonalitic gneiss at midcrustal pressures: implications for the generation of anorogenic granites, *J. Petrol.*, 1993, vol. 34, pp. 785–815.

Stacey, J.S. and Kramers, I.D., Approximation of terrestrial lead isotope evolution by two-stage model, *Earth Planet. Sci. Lett.*, 1975, vol. 26, no. 2, pp. 207–221.

Steiger, R.H. and Jager, E., Subcomission of geochronology: convention of the use of decay constants in geo- and cosmochronology, *Earth Planet. Sci. Lett.*, 1976, vol. 36, no. 2, pp. 359–362.

Stern, R.J., Neoproterozoic crustal growth: the solid Earth system during a critical episode of Earth history, *Gondwana Res.*, 2008, vol. 14, pp. 33–50.

Sun, S.S. and McDonough, W.F., Chemical and isotopic systematic of oceanic basalts: implications for mantle composition and processes, in *Magmatism in the oceanic basins*, Saunders, A.D. and Norry, M.J., Eds., *Geol. Soc. Am. Sp. Publ.*, 1989, no. 42, pp. 313–345.

Tack, L., Wingate, M.T.D., Liegeos, J.P., et al., Early Neoproterozoic magmatism (1000–910 Ma) of the Zadinian and Mayumbian groups (Bas Congo): onset of Rodinia rifting at the west edge of the Congo Craton, *Precambrian Res.*, 2001, vol. 110, pp. 277–306.

Taylor, S.R. and McLennan, S.M., *The Continental Crust: its Composition and Evolution*, London: Blackwell, 1985.

Thirlwall, M.F., Long-term reproducibility of multicollector Sr and Nd isotope ratio analysis, *Chem. Geol.*, 1991, vol. 94, no. 2, pp. 85–104.

Tretyakov, A.A., Kotov, A.B., Degtyarev, K.E., et al., The Middle Riphean volcanogenic complex of Kokchetav Massif (northern Kazakhstan): structural position and age substantiation, *Dokl. Earth Sci.*, 2011a, vol. 438, no. 2, pp. 739–743.

Tretyakov, A.A., Degtyarev, K.E., Kotov, A.B., et al., Middle Riphean gneiss granites of the Kokchetav Massif (northern Kazakhstan): structural position and age substantiation, *Dokl. Earth Sci.*, 2011b, vol. 440, no. 2, pp. 1367–1371.

Tretyakov, A.A., Degtyarev, K.E., Kotov, A.B., et al., The age of the last episode of the Precambrian regional metamorphic event in South Ulutau (central Kazakhstan): results of U–Pb geochronological studies of granites from the Aktas Complex, *Dokl. Earth Sci.*, 2012, vol. 446, no. 1, pp. 1037–1041.

Tupinamb, M., Machado, N., Heilbron, M., and Ragatky, D., Meso-Neoproterozoic lithospheric extensional events in the São Francisco Craton and its surrounding South American and African metamorphic belts: a compilation of U-Pb ages, *Rev. Bras. Geocin.*, 2007, vol. 37, pp. 87–91.

Turkina, O.M., Letnikov, F.A., and Levin, A.V., Mesoproterozoic granitoids of the Kokchetav microcontinent basement, *Dokl. Earth Sci.*, 2011, vol. 436, no. 2, pp. 176–180.

Vielzeuf, D. and Montel, J.-M., Partial melting of metagreywackes. Part I. fluid-absent experiments and phase relationships, *Contrib. Mineral. Petrol.*, 1994, vol. 117, pp. 375–393.

Watson, E.B. and Harrison, T.M., Zircon saturation revisited: temperature and composition effects in a variety of crustal magma types, *Earth Planet. Sci. Lett.*, 1983, vol. 64, pp. 295–304.

Yarmolyuk, V.V., Kovalenko, V.I., Anisimova, I.V., et al., Late Riphean alkali granites of the Zabhan Microcontinent: evidence for the timing of Rodinia breakup and formation of microcontinents in the Central Asian Fold Belt, *Dokl. Earth Sci.*, 2008, vol. 420, no. 3, pp. 583–588.

Zaichkina, A.V., Zaikanova, V.S., and Pupyshev, N.A., Precambrian and Lower Paleozoic complexes of the northwestern Balkhash Region, *Izv. AN Kaz.SSR, Ser. Geol.*, 1982, no. 2, pp. 11–20.

Zaitsev, Yu.A., Rozanov, S.B., and Filatova, L.I., *Geologiya dokembriiskikh metamorficheskikh tolshch Aktau-Mointinskogo antiklinoriya. Problemy geologii Tsentral'nogo Kazakhstana* (Geology of the Precambrian Metamorphic Sequences of the Aktau–Mointy Anticlinorium. Geological Problems of Central Kazakhstan), Moscow: MGU, 1980, part 1.

Translated by M. Bogina